Nanofluidic devices and their applications

Abgrall, Patrick; Nguyen, Nam-Trung

2008

Abgrall, P., & Nguyen, N. T. (2008). Nanofluidic Devices and Their Applications. Analytical Chemistry, 80 (7), 2326-2341.

https://hdl.handle.net/10356/94432

https://doi.org/10.1021/ac702296u

Nanofluidic devices and their applications

Patrick Abgrall and Nam Trung Nguyen

Singapore-MIT Alliance / School of Mechanical and Aerospace Engineering, Nanyang Technological University, Nanyang Avenue, Singapore 639798

Tel.: +65-6790-6174

Fax.: +65-6792-4062

E-mail: abgrall@ntu.edu.sg

Recent developments in micro- and nanotechnologies made possible the fabrication of devices integrating a deterministic network of nanochannels, i.e. with at least one dimension in a range from one to one hundred nanometers. The proximity of this dimension and the Debye length, the size of biomolecules such as DNA or proteins, or even the slip length, added to the excellent control on the geometry gives to nanofluidic devices unique features. This new class of devices not only finds applications wherever less well-defined porous media, such as electrophoresis gels, have been traditionally used, but also give a new insight into the sieving mechanisms of biomolecules and the fluid flow at the nanoscale. Beyond this, the control on the geometry allows smarter design resulting, among others, in new separation principles by taking advantage of the anisotropy. This perspective gives an overview on the fabrication technologies of nanofluidic devices and their applications. In a first part, the current state of the art of nanofluidic fabrication is presented. The second part first discusses the key transport phenomena in nanochannels. Current applications of nanofluidic devices are next discussed. Finally, future challenges and possible applications are highlighted.

Nanofluidics has been emerged as a discipline of science and engineering, where a fluid flows in structures with at least one transversal dimension approaching the nanometer range. Although, transport phenomena of fluids at the nanocale have already been studied in the past, the terminology of nanofluidics has been appearing and becoming popular only in the past few years. This growing interest stems from the new opportunities offered by micro- and nanotechnologies. While known materials such as zeolites naturally include a random network of pores, new technologies allow the fabrication of well-defined, deterministic networks of nanochannels. This was well illustrated by the works conducted in the group of Austin at Princeton (1) aiming to create an ideal porous medium, as a substitute for gel in electrophoresis. Beyond this aspect, integration of more complex functions become feasible, as it was demonstrated with the realization of a nanofluidic transistor by Gajar and Geis from MIT reported as early as 1992 (2).

Excellent reviews have been already dedicated to nanofluidics (3, 4) and the fabrication of nanochannels (5, 6). Practically, a technology is chosen according to the geometry of a device and its application. In this perspective, we choose to present the different technologies available according to geometrical parameters to assist researchers towards the most adequate choice. A second objective is to highlight the differences between micro- and nanofluidics, and the new opportunities offered by this emerging field.

According to the main objectives stated above, this perspective article consists of two parts: (i) fabrication technologies for nanochannels and (ii) nanofluidic applications. The first part aims to help readers to navigate through the large number of technological choices. The applications highlighted in the second part illustrate how nanofluidic systems and devices are powerful tools, not only to study fundamental nanoscale science but also for practical biological and chemical analysis. Finally, in the conclusion we discuss the challenges ahead and the future applications of nanofluidics.

FABRICATION TECHNOLOGIES

Definitions. Nanochannels are channels with at least one dimension in the nanoscale which is usually defined in this field as the range from 1 nm to 100 nm, while the term submicrometer has been reserved for objects in the range from 100 nm to 1 μm. Figure 1 defines the two parameters used for our classification, namely the aspect ratio (AR) between the height and the width of the cross section and the dimensionality of the channel network. Numerous nanofluidic devices are based on low AR or planar nanochannels. The term 1D (one dimensional) has also been used but may lead to confusions. Keeping the width in the micrometer scale allows the use of standard photolithography while nanometer scale in the depth can easily be obtained using well defined thin film deposition and etching methods. Planar nanochannels have also the advantage of a higher flow rate for an equivalent pressure compared to square nanochannels with two dimensions in the nanometer range and an AR close to 1. On the other hand, the fabrication of square nanochannels involves the use of specific nanopatterning techniques, which are more or less complicated and expensive depending on the dimensionality of the network. From the technological point of view, high aspect ratio (HAR) nanochannels are even more challenging, but would allow a higher level of integration and a higher throughput than low AR nanochannels.

Beyond the AR and the dimensionality, the structural material and the length will also affect the choice of the right fabrication technology. Long channels usually necessitate a very high homogeneity of the depth and are often fabricated using bonding techniques rather than time-consuming sacrificial techniques, which additionally may lead to a slight tapering (7). As for the materials, silicon is well established and benefits from the long experience gained in microelectronics over the last fifty years. Silicon dioxide channels are naturally hydrophilic and can be simply filled by capillarity. Furthermore surface chemistry of silica is well known and can be conveniently controlled using alkylsilane-based self-assembled monolayers (SAM) (8). Polymers represent an attractive alternative due to the wide range of properties available (e.g. optical, mechanical). The lower cost associated to polymer molding

techniques along with the lower price of some common polymers are also advantages for an eventual marketing of nanofluidic devices.

The simplest case: planar nanochannels. Since the lateral dimension can be defined by conventional ultraviolet (UV) photolithography, patterning of 1D and 2D networks of planar nanochannels is not a big issue. The challenge is then to avoid the collapse of very wide and shallow channels. This collapse can be due to the process itself, or other effects such as capillary and van der Waals forces. Similar situations have been encountered previously in the case of microcontact printing (μCP) (9, 10) and in the well documented problem of stiction which has been known as one of the major sources of failure of microelectromechanical systems (MEMS) and hard drives (11-13).

Bonding-based techniques. Common ways to fabricate planar nanochannels are shown schematically in Figure 2. Volkmuth et al. described a device consisting of an array of 150 nm high, 1 μm in diameter and 2 μm centre-to-centre embedded pillars as early as 1992 (1). The pillars were etched in a silicon dioxide layer and capped with a pyrex wafer by anodic bonding [Figure 2 (1)]. Han et al. reported a similar fabrication technique in 1999 (14). Channels with 1 μm depth and 90 nm depth were etched by reactive ion etching (RIE) in silicon substrate. Access holes were opened using anisotropic wet etching, an insulation silica layer was thermally grown and the channels were finally closed with a glass coverslip by anodic bonding. This approach led to structures with depths and widths of 20 nm and 5 μm using silicon-glass anodic bonding (AR of 0.004), and depths and widths of 25 nm and 50 μm using glass-glass thermal bonding (AR of 0.0005) (15).

Bonding of two glass wafers at a relatively low temperature can be achieved with anodic bonding instead of thermal bonding using an intermediate amorphous silicon layer (16). Stein et al. used adhesive bonding with a maximum temperature of 90°C to close 70 nm deep and 50 μm wide fused silica channels (17, 18). A 20 nm thick layer of sodium silicate spin-coated on the cover wafer was used as the

adhesive. Typically, using dry etching techniques, a high uniformity requires a well controlled and maintained plasma reactor. Cheaper anisotropic wet etching of silicon was shown to result in a very smooth, well controlled and homogeneous channels with straight sidewalls (19). A standard photoresist developer was used as etchant, with native oxide as a mask, resulting in a maximal depth of 500 nm and an etch rate of 3.7 $nm.min^{-1}$.

Another way to precisely control the homogeneity and the depth of the nanochannels is to take advantage of the homogeneity of the thin film deposition or growth, and the selectivity of etching. The thickness of this film is then used as a spacer [Figure 2 (2)]. Amorphous silicon (aSi) has been often reported for this purpose due to its electrical properties, the possibility to use it as an intermediate layer for anodic bonding between two transparent glass wafers and the achievable selectivity of etching between aSi and glass. Kutchoukov et al. fabricated 2 to 100 μm wide and 50 nm deep channels using aSi etched by RIE ($CF_4/SF_6/O_2$) and anodic bonding (20, 21). Schoch et al. sputtered a layer of aSi on a patterned photoresist which was later dissolved (lift-off technique) leaving a patterned aSi layer on the glass substrate without etching (22).

Low-cost, mass fabrication technologies are essential for a wide commercialization of disposable nanofluidic devices. The fabrication of square (23) and planar (24) totally-polymeric nanofluidic devices using standard embossing and bonding techniques was demonstrated. In the case of planar nanochannels, it was found that an oxygen plasma treatment was necessary before the bonding step to lower the bonding temperature below the glass transition (i.e. around 105 °C for PMMA) and to avoid the structure to collapse. The fabrication of SU-8 channels with a depth in a range of 300-600 nm and widths in a range 100 nm-2 μm have been demonstrated using a reversal imprint technique (25, 26). Replication techniques in polymers will be further discussed in the section about square nanochannels.

Sacrificial techniques. Sacrificial techniques [Figure 2 (2)] avoid eventual wafer-to-wafer alignment, bonding steps, or even planarization steps when elements such as electrodes have to be integrated. Channels with a very thin capping layer will result in a low light absorbance but are relatively fragile. It should also be noticed that integration of microchannels using sacrificial techniques is not straightforward, and paradoxically is often performed using bonding techniques (27). The first approach is to etch the sacrificial layer in liquid phase. As early as 1992, Gajar et al. demonstrated the fabrication of 88nm deep nanochannels with a length up to 0.9 mm and a widths of 10 μm using sacrificial layers (2). Using the same technique, 20 nm deep channels with a length up to 4mm and widths in the range 0.5-200 μm were reported (28). The structural layer was silicon nitride and the sacrificial layer was aSi. The etchant was TMAH heated at 75 °C or 90 °C. An etching time of 80 hours was necessary to achieve a 1.5-mm long channel with a cross section of 50 nm by 1 μm. The etching rate was observed to decrease along the nanochannels due to slow diffusion of byproducts and the small amount of fresh etchant available at the interface between the sacrificial layer and the solution. PolySi was also used as a sacrificial layer, with SiO_2 (29) and Si_3N_4 as structural layer (30). Even with the excellent etching selectivity conferred by the couple SiO_2/ Si_3N_4, the different times of exposure to the etchant along the channel lead to a slight tapering (3.2nm per 100μm of channel) (7).

In order to facilitate the release step, Foquet et al. etched irrigation holes all along the SiO_2 capping layer (31). After etching of the polysilicon sacrificial layer using a solution of TMAH (simply a photoresist developer) at 75°C, the access holes were sealed using a low pressure chemical vapor deposition (LPCVD) of a very low temperature oxide. Polyimide (PI) planar nanochannels were fabricated using aluminium as a sacrificial layer (32). A porous silicon, deposited by plasma enhanced chemical vapor deposition (PECVD) at very low temperature (e.g. 100°C or less) was evaluated as a sacrificial layer (33). The etching rate was four times higher than that of usual polySi. No details were given regarding the roughness of the layer which may be transferred in the capping layer.

Electrochemical etching represents another way to increase the etching rate. Cheng et al. released a 2 cm long nanochannel with a depth of 100 nm and a width of 300 μm within 4 min (34). Copper was etched away using a solution of copper sulfate with an applied voltage of 6V. The SiO_2 capping layer was strengthened by a polydimethylsiloxane (PDMS) sheet before the release to avoid a collapse of the structure. Despite these impressive etching rates, a drawback of the method is the necessary electrical connections of the metal lines during the etching step. The galvanic corrosion of the couple of metals Cr/Cu was also evaluated (35). The method is simpler since no electrical connections are required but leads to reduced etching rates. The commercial etchant CEP-200 was an aqueous solution of nitric acid and ceric ammonium nitrate. 100 min were required to etch 700 μm of 220 nm deep channels, independent of the width (in the range of 1 to 50 μm). The measured etching rate was ten times faster than that of the single metal. Silicon oxide, parylene, photoresist and PDMS capping layer were also tested.

Another approach is the dry etching, usually necessitating dedicated and more expensive equipment. Reported examples include the etching of polysilicon lines using XeF_2 with SiO2 as a structural layer (27). The gaseous etchant XeF_2 can isotropically etch silicon with a high selectivity versus many standard materials including polymers. Recently a high density SF_6 was used to release 300 nm thick 11 μm wide aSi structure using SiO_2 as a structural layer (36). The thermal decomposition of polymers allows releasing the channels homogeneously all along its length, overcoming the problem of mass transport of the byproducts in the channel (37, 38). Examples are later given in the following section on square nanochannels.

Top-down nanopatterning: 2D and 3D networks of square nanochannels. *Photolithography.* The fabrication of a 2D network of square nanochannels, i.e. with two dimensions in the nanorange, mostly employs the same bonding and sacrificial techniques just discussed above. The distinction then lies in the patterning techniques. The minimal resolution of the most standard patterning technique, i.e.

photolithography, is usually evaluated by the Rayleigh equation (39, 40). The half-pitch R (half the distance between the centers of adjacent features in periodic structures) is $R = k_1 \lambda/NA$, where k_1 is a process dependant factor mainly determined by the illumination conditions, the materials of the photomask, the quality of the imaging optics, and the performance of the photoresist, λ is the wavelength and NA the numerical aperture. It should be noted that the Rayleigh limit is on the pattern pitch, not on how small an individual pattern can be printed i.e. the critical dimension (CD). Thus, the CD can be much smaller than the half-pitch (or technological node). The trends in optical lithography are to reduce the wavelength λ (deep UV) and to increase the NA. NA is a proportional to the minimum index of refraction n of the imaging medium, final lens element or resist. Increasing n has led to immersion solutions where the objective is immersed in a liquid such as water instead of air.

Following the International Technology Roadmap for Semiconductors (ITRS), the half-pitch of Dynamic Random-Access Memory (DRAM) in 2007 is 65 nm and the smallest gate length is 25 nm. Actual photolithography systems in production use argon fluoride laser with a vacuum wavelength at 193 nm. The transition to liquid immersion lithography and/or to molecular fluorine lasers at 157 nm should allow reducing these dimensions further in the future but there are still many technical challenges. These projection systems have a very high-throughput, but their relatively higher prices (equipment and photomasks) prevent the use in academic research. Though photolithography has always successfully met the requirement of Moore's law and the semiconductor industry up to now, many alternative approaches are currently under investigations in order to reduce the costs and to go around its physical limits.

Serial patterning techniques. In Scanning Beam Lithography (SBL), a high-energy beam is scanned on the substrate to draw the pattern. This beam can locally modify a resist, or directly etch the substrate or even can be used to locally deposit or grow a material (41-43). This set of techniques includes LASER-based machining, Electron Beam Lithography (EBL) and Focused Ion Beam (FIB). Though exceptional

resolutions can be reached, applications of SBL to large surface patterning are still limited by the time-consuming scanning times. Femtosecond lasers are able to draw three dimensional (3D)networks in various materials such as glass or PMMA (44, 45). The minimum channel diameters in PMMA and glass were 400 nm and 700 nm, respectively. These sizes are still above the range defined for nanofluidics. The fabrication of a 2D network of 70 nm wide silicon open trenches has been demonstrated using a laser-assisted etching technique (46).

In EBL, a beam of electrons is scanned over a resist, such as PMMA. Bonds are broken in the exposed areas, which are later dissolved in a specific solvent. Structures with dimensions below 5nm have been reported (47, 48). Bonding-based fabrication of nanochannels in glass substrates patterned by EBL and RIE has been demonstrated with a resolution down to 80 nm (49-51). Sacrificial techniques have also been applied to short (typically less than a few hundred microns) square nanochannels (52). Tricks to improve the performance of sacrificial techniques include the etching of irrigation holes (53), galvanic corrosion (35) and the use of thermally degradable polymers (37, 38). Thermally degradable sacrificial layers allow releasing the structure at a rate independent of the length of the channel. Materials such as polycarbonate (PC) and polynorbonene (PNB) can be degraded at a temperature of 300 °C applied for 30 min-1 hour and at a temperature of 440 °C applied for 3 hours, respectively. It should be noted that similar polymers was developed for microchannel fabrication, with a temperature of degradation as low as 180°C applied for one hour (54).

In addition to resist patterning, FIB has often been employed for direct maskless etching, implantation or etching (43), though it should be pointed out that techniques such as LASER-induced Chemical Vapor Deposition (LCVD) and EBL also provide this direct writing capability (41, 42). FIB-based deposition is the most commonly used technique for repairing the defects on photomasks or integrated circuits. The heavier ions are less prone to scattering than lighter electrons, and theoretically result in a better resolution. Nanofluidic channels with lateral dimensions as low as 20 nm were fabricated by

milling glass or silicon substrate with a gallium-based focused beam (55, 56). Proton beams were also employed to make channels in PMMA (57).

Scanning Probe Lithography (SPL) represents a powerful tool for even smaller dimensions (58-61). As an example, this set of techniques allowed the manipulation of individual atoms on a substrate using a Scanning Tunneling Microscopy (STM) tip (62). Dip-pen nanolithography is based on the local deposition of a SAM with an Atomic Force Microscopy tip (AFM) (63). Other possibilities include the local removal of a SAM, also named “nanoshaving” (64), or the selective oxidation of the substrate with an AFM tip comprising a carbon nanotube at the end dipping in water (65). Like SBL, SPL is a serial technique and exhibits an even lower throughput, restricting its use to research or mask fabrication/repair. Parallelization was demonstrated to overcome this issue (66). Reproducibility using parallel SPL is challenging because it also depends on the substrate topography and the shape of the tip, which varies with time and use. Even though SPL seems attractive for the prototyping of ultimately small channels, only one example of an approach close to SPL has been reported for the fabrication of closed nanochannels (67).

Serial techniques demonstrate a very low-throughput. Solutions for patterning large areas includes (e.g. electron beam projection system (68) and parallel SPL (66)), but none of them is actually able to compete with photolithography at an industrial scale. However, SBL and SPL make accessible lower dimensions at the lab scale, and represent useful tools for prototyping and the fabrication of masks or templates. We will now discuss techniques alternative to photolithography to replicate a pattern starting from such masks or templates.

Replication techniques. A high resolution negative structure fabricated using low-throughput SBL or SPL can be replicated using highly parallel technologies. Many molding techniques have been invented or adapted to the micro- and nanoscale during the last ten years (61, 69, 70). Basic techniques of

imprinting are represented in Figure 3. In Nano Imprint Lithography (NIL), a thermoplastic is embossed with a mold under pressure at a temperature above the glass transition (71). In Step-and-Flash Imprint Lithography (SFIL), a UV-curable liquid precursor is imprinted using a transparent mold, making the alignment easier, and then crosslinked through UV (72) at room temperature. In reversal imprint (73), the material is first deposited on the mold, then can be transferred on various substrate. Variations exist depending on the type of deposition and transfer: polymer bonding (74), microtransfer molding (μTM) (75) and nanotransfer printing (nTP) (76). Solvent-assisted micromolding allows to pattern thermoplastics at room temperature as well (77). Using this process, the polymer is locally dissolved. A PDMS stamp wetted by an adequate solvent is used for this purpose.

This set of replication techniques has been used (i) to transfer a pattern in a resist on a substrate which is used as a mask during a subsequent etching step, or (ii) to directly imprint the structural material on the substrate. NIL has been combined with bonding-based techniques (78, 79) and surface micromachining (38, 80) to fabricate nanochannels. The templates have usually been made in silicon by EBL and RIE. Cao et al. use NIL to pattern nanochannels which were conveniently capped using a non-conformal deposition (81). Guo et al. simply imprinted a thin PMMA layer and let the silicon template glued to the substrate, instead of releasing it, to form nanochannels with dimension down to 75 nm by 120 nm (width by height) (82). Direct imprint of thermoplastic substrates have been demonstrated for the fabrication of planar (24) and square (23) nanochannels. The technology is simple, low-cost and may be applied to the mass-fabrication of nanofluidic devices. The critical issue was the bonding step, which is assisted by an oxygen plasma.

Replication by casting PDMS is widely used in microfluidics. Channels with cross-sections as small as 200 by 200 nm have been fabricated using this techniques (83, 84). Due to the low Young modulus of the material, structure suffer from collapsing as the dimensions and the AR shrinks. Solutions to overcome this issue may include the use of a ‘hard PDMS’ (h-PDMS) (85, 86). Nanochannels with a

triangular cross-section have been recently fabricated (87) using a crack-induction method (88). The triangular cross-section prevents the channel from collapsing but limits the geometry of the network.

Using reversal imprint, multiple layers can be laminated as it was done in microfluidics (89, 90). In such a 3D configuration, the thin intermediate layer between two channels may be used for valving or pumping purposes (91). Zaumseil et al. stacked layers of gold on a GaAs substrate modified with an anchoring dithiol SAM resulting in nanochannels with a cross section smaller than 100 by 80 nm (92, 93). Similar techniques have been demonstrated using PMMA (94, 95), polyethylene glycol (PEG) (96), hydrogen silsequioxane (HSQ) (70), SU-8 (25, 26) and various UV polyurethane (PU) (97).

1D network of square nanochannels. Reducing the network geometry to one dimension (network of straight and parallel lines) can make things easier. Among others, self-assembly represents a powerful set of tools to draw simple pattern at the nanoscale. As an example, the self assembly of block copolymer seems particularly well suited to this application (98, 99). Block copolymers are constituted of at least two different, immiscible polymers covalently linked. These materials evolve spontaneously in an organized structure. Depending on the ratio of each polymer, lamella, cylinder, spheres or more complicated structures could be formed. Considering a cylindrical structure, nanochannels are simply formed by selectively etching one of the components. Using a triblock copolymer, Rzayev et al. demonstrated the fabrication of 20 nm diameter and 5cm long nanochannels (100). In this case, one of the components of the copolymer was used as structural material, another one as a sacrificial material, and the last one determined the surface chemistry of the channel. An alternative approach is to use the block copolymer, after selective etching, as a mask to pattern a film or a substrate (block copolymer lithography). A technical challenge is the alignment of the structures on a long range. Solutions include the use of electric field or the preceding patterning of the substrate with different functional groups.

Structures such as carbon nanotubes (NT) are readily usable nanochannels. The challenge lies in their interconnection and their integration in a device. Though nanofluidic experiments were driven on stand-alone NT grown with an encapsulated fluid (101), on vertical NT grown on a substrate (102-104), on NT mounted at the end of the tip of an AFM (105) or on NT inserted across a polymer film (106), a planar integration is often more convenient. Riegelman et al. trapped a NT on a substrate between two electrodes by dielectrophoresis, then spin-coat and pattern a layer of SU-8 to create some reservoirs (107). Karnik et al. deposited and patterned a silicon dioxide layer on NT dispersed on a glass substrate (27).

Optical fibers or capillaries with diameters in the microscale are commonly drawn from bigger performs, taking benefit of the Poisson effect. Sivanesan et al. showed how it is possible to shrink the dimension of a PC microchannel from 20-30 μm down to 400 nm by heating and pulling the thermoplastic (108). In electrospinning, the material is drawn by the applied electric field between a needle and the substrate. Using such fibers as a sacrificial material, it was possible to fabricate channels with elliptical cross sections as small as 75 by 50 nm (109, 110). Wang et al. extruded coaxial fibers made of a mixture of a silica sol-gel and motor oil (111). Nanochannels with an inner diameter of 20 nm were formed after annealing and elimination of the oil. Using a technique pioneered by Evans et al. (112), a micropipette was pulled away from a lipid vesicle to form networks of lipid bilayer channels with an inner diameter of 50-150 nm (113-115). Actuation of these biomimetic channels using moving walls and other functions have been demonstrated (116-118). Similar techniques have been demonstrated by pulling a more robust cross-linkable polymer with a micropipette or optical tweezers (119), or by drawing a sacrificial polymer with an AFM tip (120).

Collapsing of a nanochannel is usually an issue, but one can also take advantage of it. Pearson et al. described a self-sealing technique where nanochannels are formed by collapsing of two resist lines (121). Also to order a bonding step, a trench can also be conveniently sealed using a non-conformal

deposition. Examples of reported non-conformal deposition include LPCVD, PECVD, inclined evaporation or sputtering of SiO_2 (53, 81, 122, 123), the PECVD of parylene (124) and the evaporation of gold (123). Recently, Chen et al. demonstrated a similar sealing technique using wet oxidation starting from well designed trenches (125). Oxidation may also be used to shrink the dimensions of channels (122, 126).

Edge lithography is a set of techniques taking advantage of the asymmetry at the edge of a step to pattern structures. The 'step lithography' lithography technique depicted in Figure 4(1) was patented by Texas Instruments in 1980 (127). Tas et al. employed this technique to pattern sacrificial polySi nanowire and fabricate nanochannels (128). Using a trench refilling technique and a planarisation by chemical-mechanical polishing (CMP), Lee et al. convert the thickness of a SiO_2 film into the width of nanochannels which were later sealed by a non-conformal deposition (123). A well controlled under-etching (129), as shown in Figure 4(2), was used to fabricate 10 nm high and 200 nm wide nanochannels (122). The Si_3N_4 surfaces were oxidized using an oxygen plasma before sealing to ensure homogeneous surface properties.

Phase shift lithography (PSL) can also be considered as an edge lithography technique. Along with optical proximity correction and off-axis illumination, PSL is one of the resolution enhancement technologies enabling subwavelength optical lithography (130). Phase-shift photomasks are fully transparent masks including trenches with a depth $d = \lambda/[2\ (n-1)]$ where n is an integer. At the edge of a step, the phase shift between the light going through the mask material and the light going through the air results in a destructive interference. Elastomeric phase shift masks have many advantages over the glass ones, such as their very simple and fast production, their low cost and their conformal contact during the exposure (131). Resolution down to 30 nm was demonstrated using this technology (132). It was shown that the resolution in near-field PSL (i.e. in contact mode using elastomeric phase masks) is strongly dependent on the spacing between the patterns, indicating the method is best fitted for drawing

isolated objects (133). Using these stamps in proximity mode can result in a complex intensity distribution (134). This technique was applied to the fabrication of 3D nanofluidic filters in SU-8. Interference lithography is another optical lithography enabling parallel patterning of simple nanostructures (135). Basically, a photoresist is exposed to the interferences of two inclined coherent light beams. The fringe to fringe period T of the intensity pattern is given by $T = (\lambda/2) \sin(\theta/2)$ where θ is the angle between the two waves. IL is more costly and more difficult to implement than near-field PSL but allows a higher density of lines or dots with an easier control of the dimensions. IL was applied to the direct fabrication of nanochannels (125, 136) and to create templates for replication (81, 97). A 3D IL technique was also demonstrated for the realization of 500 nm diameter tubes in PDMS employing a sacrificial method (137).

HAR nanochannels and nanopores. Pushing a liquid at a reasonable flow rate in a long nanochannel usually lead to excessive pressures, which are not compatible with most of the fabrication techniques. Scaling laws benefit more to electrokinetic- and capillary driven flows which are actually the most common techniques to run a liquid in a nanofluidic chip. For many applications a dense array of HAR nanochannels would be an optimal choice when a higher flow rate and/or a pressure-driven flow are required.

Only a few groups reported the fabrication of HAR nanochannels. O'Brien et al. realized 500 nm high and 50 nm wide channels by combining IL, RIE in silicon and anodic bonding (136, 138). Mahabadi et al. demonstrated the fabrication of 5 μm high and 200 nm wide channels using proton beam writing in PMMA (57). Other techniques were employed for the fabrication of HAR nanotrenches and can be applied to nanofluidics. The trench refilling technique is another edge lithography technique which combines bulk and surface micromachining (139). A thin sacrificial layer is deposited in a trench etched by DRIE in silicon. Then the trench is filled, and the sacrificial layer is etched. Trenches with a width of 80 nm and a height of 20 μm were obtained (140). Employing a similar technique, Martin et al.

fabricated 7 nm wide and 3 μm high open channel corresponding to an AR of 430 (141). A nanotrench with an AR of 125 was etched in silicon using a photo-assisted electrochemical etching technique (142). EBL and an inductively coupled plasma (ICP) source were used to etch a 3 μm high and 200 nm gap (143). Pourkamali etched 130 nm wide trenches with an AR of 20 (144). Anisotropic wet etching was also investigated (145).

Nanopores can be defined as very short (i.e. 10 μm or less) nanochannels. Their diameters are usually on the order of the nanometer, tailored for single-strand DNA. Interested readers may refer to a recent review by C.Dekker (146). α-haemolysin is a transmembrane protein forming nanopores with a diameter of 1.4 nm. These biological pores can spontaneously insert themselves through a lipid bilayer, similar to a cell membrane (147). To increase the stability and to further tune the channel size, various alternative techniques have been developed, based on the etching of insulating membranes. Nuclear track etching (148), ion beam (149) and electron beam (150) have been used to fabricate 'solid-state' nanopores with diameters down to 0.8 nm (151). It was demonstrated that is possible to finely shrink or enlarge these solid-state pores using an adequate ion or electron beam.

APPLICATIONS

Transport phenomena in nanochannels. *Electrokinetics.* The first question arising is: what is so different in a nanochannel compared to a macro- or even a microchannel? Readers familiar with microfluidics already know some specificities of liquid flow at the microscale such as the laminar flow or the high surface to volume ratio making electrokinetic, capillary or heat transfer effects particularly important, among others. Let us focus first on electrokinetics. Figure 5 illustrates the concept of an electrical double layer (EDL). Most surfaces submerged in an aqueous solution gain a net charge density which may originates from chemical reactions (e.g. protonation or deprotonation), adsorption or defects in a crystalline structure (152). Surface charges can also stem from an external electrical potential. In the liquid, these charges are shielded by a layer of adsorbed ions, the Stern layer, and a mobile layer, the diffuse layer. The zeta potential ζ is the electric potential at the shear plane between these two layers.

The EDL is composed of the Stern layer and the mobile layer. The screening length is named the Debye length λ_d. As a rule of thumb for a symmetric electrolyte in water at 298K, λ_d *[nm]* $\approx 9.6/(c^{1/2} z)$ where c is the electrolyte concentration in mM and z is the valency (152). So, in these conditions and considering a monovalent electrolyte, λ_d is in a range of 0.1-100 nm for a concentration ranging from 0.01 to 10 mM.

In a microchannel, λ_d is small compared to the typical dimensions and, without an external field, the electric potential is neutral almost everywhere in the channel but at the liquid/solid interface. As depicted in Figure 6, the situation is different in a nanochannel. As the dimensions are shrunk down (and/or the ionic concentration is decreased), the EDL occupies a non-negligible fraction of the channel and the quantity of surface charges becomes comparable to the quantity of charges in the bulk electrolyte. Due to the electroneutrality requirement, the ratio of counter-ions to co-ions in the channel is becoming larger and larger, and the electric potential is not neutral anymore. These phenomena are at the origin of the Donnan or co-ion exclusion effect well know in semi-permeable membrane technologies (3, 153). They also explain the higher conductivity observed at low salt concentration in nanochannels, the influence of the surface treatments on it (4, 17, 22, 154-156), and other charge-selective effects (157, 158). Several articles have reported models of the EDL in a nanochannel (159-163).

These differences between micro- and nanochannels have important consequences for electroosmosis. Electroosmosis is a well-known method to drive a fluid in microchannels by simply applying voltages in the reservoirs. The electroosmotic velocity in the bulk V_{EOF} is given by the Helmholtz-Smoluchovsky equation $V_{EOF} = (E\,\varepsilon\,\varepsilon_0\,\zeta)/\eta$ where E stands for the applied electric field, ε the relative dielectric permittivity, ε_0 is the vacuum permittivity and η the dynamic viscosity of the electrolyte. Many applications in microfluidics and analytical sciences, such as capillary electrochromatography (CEC), an electroosmosis-driven version of high performance liquid chromatography (HPLC), benefit from the low dispersion generated by the plug-like velocity profile of electroosmosis. However, considering a

nanochannel whose smallest dimensions are close to λ_d, the electroosmotic flow rate in a nanochannel is reduced compared to its value in a microchannel, and its profile is no longer flat (4, 164, 165). Electroosmosis was observed in nanofluidic devices (32, 57, 126). Streaming potentials and currents induced by a pressure-driven flow have also been measured in nanochannels (166). Molecular dynamic simulations predicted some differences with continuum models for channels close to the nanometer scale (167-171).

Capillary effects. The Laplace pressure P_L arises at the interface of any two-phase system. P_L equal to $\gamma\ (1/R_1+1/R_2)$, where R_1 and R_2 are the principal radii of curvature and γ is the surface tension of the liquid in air. Simple trigonometry leads to $P_L = 2\ \gamma\ cos\ \theta_c/r$ in the case of a cylindrical capillary, where θ_c the contact angle of the liquid with the channel walls. In the case of a planar nanochannel, where the depth d is much smaller than the width w, the approximation $r \approx d$ may be used. Applying this equation, it can be noted that the capillary pressure can locally reach very high values at the nanoscale. Considering water with a surface tension of 72.8 mN/m and channels with a diameter 10-100 nm having a hydrophilic surface (θ_c=50 º), the capillary pressure is approximately in the range 10-100 bar. Considering now a hydrophobic surface (θ_c=105 º), the driving force has an opposite direction (towards the inlet of the channel), and is in a range 4-40 bar, indicating that relatively large pressures would be required just to fill hydrophobic nanochannels. As a consequence of these simple considerations, a water plug surrounded by air at atmospheric pressure in an hydrophilic nanochannel is at a negative pressure (29). This negative pressure induced a bending of a thin enough capping layer, resulting in a curvature of the meniscus at the interface air/liquid. A negative pressure of 17 +/-10 bar was deduced from the shape of this meniscus. The absence of cavitation was explained by the fact that the height of the channel was smaller than the critical radius necessary for a bubble to expand under these conditions.

Combination of the Laplace pressure with the Poiseuille equation and integration leads to the Washburn equation (172). The position of the meniscus x is equal to $\sqrt{D}.\sqrt{t}$, where the filling

coefficient D is $\gamma \cos \theta_c r/(2 \eta)$ for cylindrical capillaries and $\gamma \cos \theta_c d/(3 \eta)$ for planar channels (considering that for $d << w$ the Poiseuille number is 24). Experimentations on capillary driven-flow at the nanoscale showed deviations from this classic relation at the nanoscale (50, 173-177). Sobolev et al. measured the capillary filling process of water in quartz capillaries with radii ranging from 40 to 200 nm (173). They reported a slower filling speed, which would correspond to an increase of the apparent viscosity of 40% compared to the bulk value, for small filling speeds. This singular behavior rapidly vanishes as the radius increases. According to the authors, these results may be explained by the adsorption of a film on the dry surface ahead of the moving meniscus affecting the dynamic (wetting) contact angle. Hibara et al. and Tas et al. reported similar results (50, 174). The later argued that this slowdown may be due to an electro-viscous effect (a counter electroosmotic flow induced by the streaming potentials), already predicted by Burgreen and Nakache in 1963 (164). It was shown that the filling rate tended to its usual value when the concentration of salt was increased, so when λ_d was decreased, what is in accordance with this hypothesis. Intriguingly, the same group recently reported a reduced filling speed for ethanol and an increased filling speed for water in 6 nm deep channels (176). In this later device, the filling kinetics was monitored via a microfabricated Fabry-Pérot interferometer, consisting in two embedded mirrors at the top and the bottom of the planar channel. Using glass nanochannels with sharp corners, the importance of the corner flow on the drying rate was experimentally demonstrated (178). This example illustrates well how nanofluidic devices can be used to investigate a wide range of phenomena. Recently, enhanced capillary filling speed were reported in a nanochannel, due to the bending of a the thin capping layer induced by negative pressures in the liquid close the interface (179).

Slip length. The no-slip boundary condition in fluid mechanics has often been argued throughout history (180, 181). Recent experiments have demonstrated slip lengths up to a few microns on superhydrophobic surfaces (forest of hydrophobic carbon nanotubes) (182). A slip length similar to the typical dimension of the channel would result in an amplification of the pressure- or electroosmotic-

driven transport (181, 183, 184). A large enhancement of the mass transport through carbon nanotubes has recently been reported (185, 186). However, due to the very large capillary pressures developed during the introduction of a liquid in a hydrophobic nanochannel, priming of these structures could be a serious challenge.

Routing, preconcentration and separation of ions and biomolecules. The proximity of the typical dimension of nanochannels and the size of biomolecules, such as DNA or proteins, make nanofluidic devices powerful tools for genomics or proteomics (187, 188). Though well established, high-throughput genotyping techniques are now routinely used, micro- and nanofluidic chips may be a complementary way to further reduce the costs and reach the target of the 'thousand dollar genome' which would, among others, drastically improve the diagnostic and the early detection of eventual predisposition to diseases. As the 13-year long Human Genome Project has ended, efforts are growing to study the genes expression, proteins. In contrast to the genome, the proteome not only changes from one individual to another but also evolves during the time. Consequently the 30 years old technique of 2D gel electrophoresis has to be replaced by better and faster separation tools to analyze these tiny changes and track their evolutions (189). There may also be room for micro- and nanofluidics.

Sieving mechanisms. Basics on sieving mechanisms of chain-like biomolecules have to be given for a better understanding of the operation of nanofluidic devices. Though a few elements are given in this part, a complete discussion on this difficult topic is largely beyond the scope of this perspective. Interested readers can refer to the review articles on electrophoresis from Viovy or Slater (190, 191). In addition to the electrostatic sieving effects described in the previous section, steric and entropic sieving mechanisms occur in nanochannels (192, 193). Three mechanisms are schematized in Figure 7. The electrostatic sieving mechanism is predominant when λ_d is similar or larger than the typical dimension of the channel (Figure 7, (a)). As λ_d becomes negligible, steric and entropic effects become predominant. Ogston sieving (Figure 7, (b)) occurs for molecules smaller than the channel. Fewer conformations and

orientations are possible for a flexible chain-like molecule in a confined space, resulting in a loss of internal entropy. As a consequence, smaller molecules (i.e. with less possible conformations) have a higher transport rate.

Larger molecules have to unfold, decreasing their entropy, to enter a channel slightly smaller than their diameter of gyration. The chain is trapped outside the constriction where it maximizes its conformational entropy, leading to the term 'entropic trapping' (194, 195). Thermal agitation may allow a loop to escape the entropic trap, Figure 7, (c). A loop long enough can pull the whole molecule inside the channel under the action of an electric field. Surprisingly, and opposite to the behavior in a gel, larger molecules have a higher transport rate through planar channels (i.e. with a rectangular cross-section) than smaller molecules (14, 196). This was explained by the larger contact area between a larger molecule and the rectangular slit, resulting in a higher probability to form a loop and escape. Finally, a chain already confined in a network of obstacles much smaller than its radius of gyration advances like a snake following the reptation model.

Routing and preconcentration. By taking advantage of electrokinetic mechanisms, gating or sorting of molecules has been demonstrated. Kuo et al demonstrated the control of the transfer of an analyte from a microchannel to another (injection and collection) through a nanoporous membrane (197). This highly accurate dispensing method was applied to the fabrication of a Pb^{+} sensor (198) and to the study of the kinetics of the heterogeneous reaction between organomercaptan and colloids of gold (199). Schoch et al showed how the pH affects the diffusion of proteins in a nanochannel, which was maximal when the molecules were neutral at their pI (200). It can be noted that nanofluidic chips has also recently been used as platforms to measure diffusion coefficients of fluorescently-labeled molecules through a nanochannel (201). As it will be detailed in the section concerning nanofluidic electronics, the sign and density of surface charges can be controlled by surface treatments and/or an electrostatic field. This property has been used to actively control the concentration of ions (2, 27) and the routing of proteins

(202) in nanofluidic circuits. Efficient preconcentration schemes are often desirable to increase detection capabilities in lab-on-chips. The interface between micro- and nanochannels have been used to agglomerate molecules (using entropic or electrostatic effects), resulting in a concentration (up to a factor 10^6) (203-206). This has been recently used to improve the kinetics of immunoreaction, which is limited by the diffusion at low concentrations (207).

Free-solution separation. Size separation of DNA is central in molecular biology. Applications include sequencing, DNA finger printing or restriction mapping. Conventional slab gel electrophoresis loses its efficiency for molecules larger than 20 kbp (208). Separation of larger DNA (up to 10Mbp) is commonly performed by pulsed field gel electrophoresis (PFGE) (209). However, the technique is very time-consuming (runs take 10 to 200 hours). Pulsed field capillary gel electrophoresis (PFCGE) overcomes some of these problems (210, 211), but suffers from a lack of reproducibility due to the aggregation of large DNA fragments under strong electric fields (212), and requires a more complex and expensive instrumentation than slab gels. Though the free-solution mobility is independent of the DNA molecular weight N for values larger than 400bp and monotonically decrease with decreasing N for smaller fragments (213), recent experiments in nanochannels revealed intriguing properties. Cross et al. reported a size-dependant mobility for DNA in the range of 2-10kbp in 19 and 90nm deep channels, scaling as $N^{-1/2}$ (214). This was attributed to interactions with the solid walls. Higher mobilities than expected have been reported during the free-solution electrophoresis of rod-like DNA molecules (smaller than 100bp) in nanochannels at low ionic concentrations (215).As explained in previous sections, (i) coions in a nanochannel are repelled from the wall and (ii) the velocity profile of an electroosmotic flow is no longer flat, i.e. particles separated from the walls by different distances have different velocities. Pennathur and Santiago took benefit of these two features to realize a separation by valence (165, 216). Both ionic valences and mobilities were accessible by comparing separation results in micro- and nanochannels.

Shear-driven separation. An alternative method to drive a flow in a nanochannel is to apply a shear by axially moving a substrate separated from another by a spacer (217). A first advantage of this method is to not involve very large pressures as for pressure-driven flows. Additionally, shear-based actuation does not rely on the electrolyte (which may be incompatible with some biological processes) and the often inhomogeneous surface charges as for electrokinetic-driven flows. Finally, reaching the optimal velocity for a chromatographic separation is not always possible using only slower electrokinetic effects. Separations of dyes (217, 218) and peptides (218) were demonstrated in less then 0.2 s over a distance of only 1.8 mm. While shrinking the dimensions of the channels increases the separation speed, the detection of fewer and fewer molecules was identified as a challenge which may be solved by continuous-flow separation devices, as discussed above, but also by advanced fluorescence techniques or the integration of more sensitive sensors.

Batch separation in a nanopatterned matrix. Ideal, deterministic porous networks have been shaped using micro- and nanotechnologies as a substitute to porous gels (1). These model porous media have first been used to study the transport of DNA. By taking advantage of the added degree of control on the design, they have also allowed new separation schemes. An example is the device introduced by Han and Craighead, whose consists of alternating deep and shallow channels (14). The separation of long DNA molecules (i.e. 5-200kbp) within 30 min by entropic trapping (molecules larger than the pores) have been demonstrated (14, 196, 219). A similar device was employed for the separation of proteins and smaller DNA molecules (i.e. less than 1000 bp) by Ogston sieving (220, 221). A simple array of nanopillars is prone to clogging with large molecules, which may also break up after hooking on a structure. Baba et al. solved these problems by introducing another design on the basis of size exclusion chromatography (SEC) (222). The array consists in wide channels parallel to the flow connected by perpendicular narrow channels. Large molecules were excluded from the narrow gap, and moved smoothly through the wide channels. Due to Brownian motion, smaller molecules able to enter the narrow gaps traveled a longer path, leading to the size separation. Bakajin et al demonstrated the

separation of 100kbp DNA in 10 s by switching electric fields along two directions in a nanopillars array (204). Briefly, longer molecules spent more time going back and forth in a same path during a period, entangled around the posts. It can also be noted that, at the microscale, separations by CEC and HPLC have been demonstrated in microfabricated colums (223, 224).

Anisotropic continuous flow separation. Continuous flow separations in microfluidics have been well reviewed in a recent article (225). Techniques such as free-flow electrophoresis (226) or free-flow isoelectric focusing (227) allow a continuous injection and collection of the samples, making easier the system integration. Real-time monitoring become possible and integration of the signal over the time would allow overcoming detection limits. While standard electrophoresis gels are isotropic porous media, the recent progresses in fabrication allow patterning anisotropic nanostructures array. Duke and Austin proposed an array of oblong obstacles designed in such a way that smaller, more diffusive species have a higher probability to be deflected in one direction than larger molecules (228). Using this principle of rectification of the Brownian motion, separations of DNA with sizes in a range 15-167 kbp were achieved (229-231). The resolution of the method is limited by its statistical nature. The “DNA prism” is the continuous flow version of the method using alternating fields in a hexagonal post array described in the last section. It has been demonstrated to perform separation of DNA with sizes in a range 61-209 kbp within 15 s (232). Hattori et al designed a bi-forked junction where the access to the main channel (i.e. with the lower hydraulic resistance) was restricted by an array of nanopillars (233). Smaller molecules predominantly flowed in the main channel while bigger molecules were deflected in the side channels. The laminar flow inside an array of nanostructures leads to multiple fluid streams which do not mix. Considering a flow rate high enough to minimize diffusion effects, the streamline followed by a particle around a pillar depends on its size (i.e. how far is its center from an obstacle). The method named “deterministic lateral displacement” is based on this statement, and has been applied to the separation of long DNA molecules (61 and 158 kbp) (234). It is interesting to note that the resolution increase with higher flow rates, opposite to the method based on the rectification of the Brownian

motion. Fu et al recently extended the concept of alternating deep and shallow regions (described in the previous section) to a 2D array (193). The device consisted in an array of deep channels connected by shallow nanoslits. Through the application of a diagonal electric field, DNA or proteins jump more or less frequently (depending on their size and the sieving mode) from one deep channel to another, leading to different trajectories.

Single molecule analysis. As the dimensions are shrunk down, less and less molecules are present inside the volume defined by the nanochannel. Smaller probe volumes allow enhancing the spatial resolution of sensing techniques (235, 236). Similar to two-photon excitation methods, confining a liquid in a nanochannel is a way to obtain very small probe volumes. An ultimate goal is to handle and probe individual biomolecules, giving access to statistical distributions, instead of measuring values averaged on large and sometimes heterogeneous populations. Such approaches may give a deeper insight on fundamental phenomena.

Nanofluidic devices have been ideal platforms for biophysicists to study and test the models of the motion of individual DNA molecules in a porous media evocated in the previous section (1, 49, 78, 79, 237-241). Using fluorescence correlation spectroscopy, Foquet et al. were able to directly count and measure the length of DNA fragments (31). Riehn et al. demonstrated restriction mapping of DNA by stretching the molecules in nanochannels (51). Also using high resolution fluorescence microscopy techniques, Wang et al. studied the interaction of DNA with a protein by directly counting the number of proteins bound to DNA (242). Increasing the persistence length of DNA molecules by reducing the ionic strength of the buffer increased the minimum dimension of the channel required to stretch DNA molecules (243). This allowed using simple PDMS casting techniques to produce channels with a crosssection of 100nm by 1 μm which were small enough to extend DNA. Recently, Krishnan et al reported that DNA molecules, introduced by capillary filling, spontaneously extend at the edges of a planar nanochannel, introducing a simple solution to stretch DNA (244). The origin of this attractive

potential remains unclear. Reisner et al. reported longer extension of DNA than expected in a nanochannel, due to the interactions between the molecule and the walls (245).

Obviously, the selection of fluorescent labels is very important for single molecule studies by fluorescence. Owing to their exceptional brightness, quantum dots and nanodiamonds are very promising for this purpose (246, 247). Though single molecule studies are at present largely restricted to optical techniques, an electric, label-free, method of detection would be easier to integrate in a chip. Recently, Zevenbergen et al. demonstrated the integration of such a method, named redox cycling (36). In their device, two facing electrodes were integrated at the top and the bottom of the nanochannel. By applying adequate electrochemical potentials, the products generated at one electrode became reactants at the second electrode. While electrochemical reactions normally involve one or a few electrons making single molecule detection virtually impossible, redox cycling allows each molecule to contribute multiple electrons to the induced current. An amplification factor of 400 and a promising resolution of 70 molecules were measured.

The translocation of individual molecules through a nanopore has also been a rapidly expanding field for the last ten years (146, 248). Fabrication of biological and solid-state nanopores was briefly discussed in a previous section. Translocation has also been demonstrated in a device constructed around a NT (249). Figure 8 schematically presents how a very small pore can be used to get informations about an individual molecule. The DNA strand is moved through the nanopore under an applied electric field. When the DNA enters the pore, the electric current drops, given that a part of the volume of electrolyte inside the pore is replaced by the macromolecule. Thus, by monitoring the current, one would observe a series of downwards peak. Each peak (Figure 8 (a)) indicates that a DNA strand traverses the nanopore. If the pore is small enough (less than 10nm for a double-stranded DNA and 2nm for a single-stranded DNA (250)), the molecule will be stretched and transferred trough the pore in a linear fashion. The length of DNA may then be deduced from the duration of a translocation event. This

approach for sizing was demonstrated using solid-state nanopores (251). However, it was revealed that molecules traveling through biological nanopores have different velocities depending on the relative quantity of bases (A, C, G or T) (252) or the orientation (3’ or 5’) (253), eventually indicating that further efforts are required to better understand the underlying physics and fully take benefit of these devices. To answer some of the questions on the translocation, Keyser et al. has used optical tweezers on a bead attached to the DNA strand for direct force measurements (254). Finally, information about the bases may be extracted from transversal electrical measurements during the translocation (255-257). Integration of elements such as electrodes in the nanopores may give a new way to read the sequence of DNA as it can be done with a magnetic tape in a tape deck (Figure 8 (b)).

Nanofluidic electronics. A common solid-state diode is a junction between a n-type semiconductor, where most of the charge carriers are electrons, and a p-type semiconductor, where the charge carriers are holes. In nanofluidics, as stated above, the mobile charges in the electrolyte are controlled via the fixed surface charges. This possibility to control the nature of the mobile charges inside the channels led to the idea of nanofluidic diodes and transistors (258), or, more generally, to the concept of nanofluidic electronics (259). Instead of the diffusion or ionic implantation processes employed in microelectronic fabrication, the doping of nanofluidic electronic devices can be obtained through chemical modifications of the surface (17, 154, 156) or by applying an electrostatic field though integrated electrodes (260, 261), similar to a field-effect transistor. Obviously, the objective is not to compete with the well established semiconductor technology. The ionic mobility in dilute electrolyte is more than a million times lower than either the hole or electron mobility in silicon, which is a clear disadvantage for high-speed electronic devices (262). However, the possibility to control the flow of chemical and biological species, and realizes logical operations with, offers many very exciting opportunities in term of process automation, and may lead to the rise of a new class of devices in the coming years.

In microfluidics, it was demonstrated that the zeta potential (and the resulting electroosmotic flow) can be controlled by an external and transversal electric field (260, 261). Using the same technique in nanofluidics, the ionic concentration in the whole nanochannel can be modulated. As early as 1992, Gajar et al. demonstrated a nanofluidic transistor, called 'ionic liquid-channel field-effect transistor' (2), based on this principle. The anion/cation concentration ratio increased by a factor 17.2 when the gate voltage was changed from 0 to 25V, corresponding to an increase of conductance by a factor of 5.2 using a solution of KCl in glycerol. Recently, Karnik et al. reported a similar device, which was use to control the transport of proteins (27, 202). Stern et al. proposed a chemical charged coupled device able to concentrate and separate, by moving packets of ions along a nanochannel integrating a batch of sequentially-biased electrodes (28). By correctly adjusting the stepping frequency, the device was expected to separate smaller ions from bigger ions, unable to follow at a too high rate of transfer. Unfortunately, the fabrication of the device presented some technical issues, probably due to the too high residual stress, and has not been tested. Fan et al. highlighted the analogy between doping and surface treatment in nanofluidic transistors by reversing the polarity of a nanofluidic transistor (156). This property may allow monitoring the binding of species at the surface of the channel for biosensing applications (154).

Nanofluidic diodes have recently been demonstrated using different technologies. Karnik et al. employed a technique named diffusion-limited patterning to create junction in silica nanochannels realized using sacrificial techniques (263, 264). The diffusion-limited patterning consists in sequentially injecting two reactants in the reservoirs. During their diffusion, the reactants bind to the channel surface. The pattern is then controlled by the respective time of diffusion. Vlassiouk et al. used track-etched PET membranes (265). Half of the conical nanopore was coated with positive amino group, while the other half presented negatively charged carboxyl groups. Both groups reported a rectification effect. Surprisingly, Karnik et al. reported that this rectification effect vanishes at low concentrations (KCl solutions below 1mM) and that the ionic current is less than expected. It is worth to note that

rectification, with less efficiency, was already observed in homogeneously charged conical nanopores (148, 266-270). Recently, Miedema et al engineered a nonrectifying biological porin into a ultimately small nanofluidic diode (271). The protein was designed to include spatially separated regions of opposite charge.

Others. Apart from these mainstream applications, nanofluidics may have a lot to offer in various areas. Drug delivery devices have been designed to slowly diffuse a drug in vivo (272, 273) The ability to control the size and the geometry of nanopores allows an excellent control of the diffusion kinetics. Photonic devices often require structures with dimensions in the order of a few hundreds of nanometers. Erickson et al. combined a 2D photonic crystal with a nanofluidic channel (84). It was possible to dynamically adjust the photonic properties by filling the structure with solutions of different refraction indices. Gersborg-Hansen and Kristensen used an array of channels as a resonator for a dye laser (274). Kameoka et al. realized and tested a refractive index sensor based on photon tunneling (16). Based on the streaming potentials, it has been shown than a conversion from hydrostatic to electrical energy is possible in nanochannels with a theoretical maximum efficiency of 12% using aqueous-based solutions of lithium ions (166, 275-277). First experiments led to an efficiency of only 3% (278). It was recently pointed out that increasing slip length would improve this efficiency (279). As described in the section regarding electrokinetics, the transport of counter-ions is enhanced in a nanochannel. Taking advantage of this effect, Liu et al. proposed to use an array of nanochannels as the membrane of a fuel cell to enhance the transport of protons (280). These are typical integrations where the integration of a high density of HAR nanochannels would be attractive.

CONCLUSIONS

In the first part on the fabrication technologies, different techniques were critically discussed according to the aspect ratio of nanochannels and the dimensionality of the nanofluidic network. Though arbitrary 2D network of planar nanochannels (i.e. having only one dimension in the nanoscale) can be realized using photolithography and relatively simple micromachining techniques, fabrication of square

nanochannels (i.e. having two dimensions in the nanoscale) requires specific nanopatterning techniques (i.e. slow serial techniques such as FIB or EBL). These slow serial techniques can be combined with parallel replication methods (e.g. NIL) to improve their throughput. It has been shown that numerous alternative techniques exist to fabricate a 1D network of straight square nanochannels. A combination of these alternative techniques with more standard top-down lithography tools may be an elegant solution to pattern arbitrary 2D networks. Finally, fabrication of ultimately small nanopores and also HAR nanochannels for very dense, high-throughput systems has been discussed.

Due to the very slow mass transport of the etchant in a confined space, bonding-based techniques seem to be more suitable to the fabrication of nanofluidic devices, especially with long channels, than sacrificial techniques. The transition from silicon or glass technologies to cheaper polymer technologies seems to be a necessary step to make disposable nanofluidic devices commercially viable. It was shown that the lower Young's modulus of these materials make this approach more challenging, especially for the bonding of wide and shallow planar nanochannels, but is possible. However, in some specific cases such as when the integration of electrodes is required, sacrificial techniques may be considered as an interesting alternative (e.g. to avoid a polishing step). The use of electrochemical etching and thermal decomposition of sacrificial layers are possible ways to enhance this process.

Nanofluidics is promising in many applications where a random network of pores (electrophoresis gel, porous membranes) could be advantageously replaced by a well defined, deterministic network of nanochannels. Due to the dramatic surface to volume ratio, it has been shown that transport phenomena in nanofluidics are different from what is known at the macro- and even at the microscale. The proximity of at least one of the dimensions of a nanochannel and the Debye length, the slip length or the size of many biomolecules leads to many fascinating effects specific to the scale 1-100nm. As the channel size and/or the ionic concentration are reduced, the concentration of mobile ions in the electrolyte becomes dependant from the fixed surface charges. These steric and electrokinetic effects,

associated with a high level of control over the geometry, led to innovative concentration and separation devices. The confinement makes possible the handling and the detection of single molecules, making nanofluidics an extraordinary tool for biophysicists. Patterning the surface chemistry has resulted in nanofluidic electronic devices where holes and electrons are replaced by cations and anions, paving the way to chips able to realize complex and automated chemical or biological operations. Finally, some applications in drug delivery, optofluidics and energy conversion were presented.

Obviously, further efforts are needed to address the intriguing behaviors reported. Examples include the capillary filling slowed down at the nanoscale, or the anomalous electrostatic interactions between DNA molecules recently described by Krishnan et al (244). According to molecular dynamics simulations, new phenomena may arise as the dimensions are coming closer to the nanometer. A better understanding of the mass transport at the nanoscale will be a key for the design of future devices. Owing to their deterministic geometry, nanofluidic chips are also ideal platform for these studies, shedding light on the mechanisms occurring in random porous media. From the end users' point of view, experience has shown that often end-users simpler tools are preferred to more efficient but less convenient solutions. A typical example is the slab-gel electrophoresis still widely used by biologists while many faster and better alternatives have been developed. The integration of the nanofluidic building bricks reported in this perspective in a complete lab-on-chip is a key point for this technology to reach its full capability.

ACKNOWLEDGEMENTS

The authors acknowledge the support of the Singapore-MIT Alliance, flagship research project "Design-Simulate-Fabricate Micro/Nano-fluidics for Cell and Biomolecule Manipulation" and the joint French-Singaporean "MERLION" program.

FIGURES

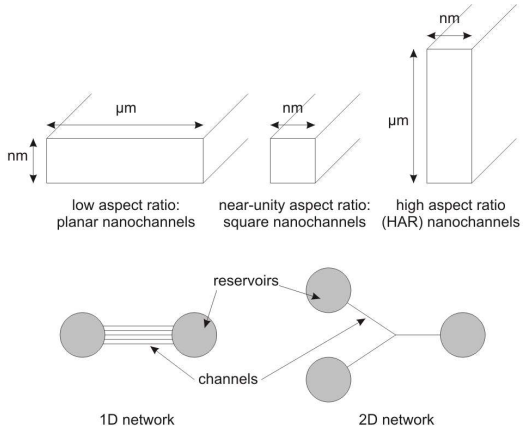

Figure 1. Geometrical definitions used in this article: 1D and 2D networks of planar, square and high aspect ratio (HAR) nanochannel.

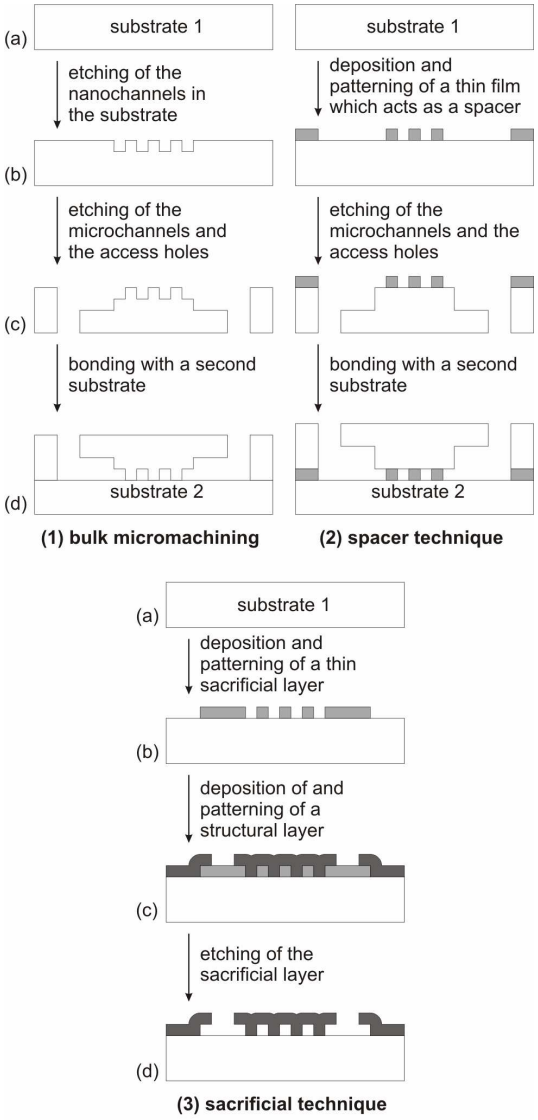

Figure 2. Fabrication of planar nanochannels in silicon/glass technology. (1) bulk micromachining: nanochannels (b), microchannels and access holes (c) are etched in the substrate, then closed by a second substrate (d) (1), (2) spacer technique: a thin layer is deposited and patterned (b), microchannels and access holes (c) are etched in the substrate, then closed by a second substrate (d) (20) and (3) sacrificial technique: a thin layer is deposited and patterned (b), a structural layer is deposited and patterned, then the sacrificial layer is etched away (d) (2).

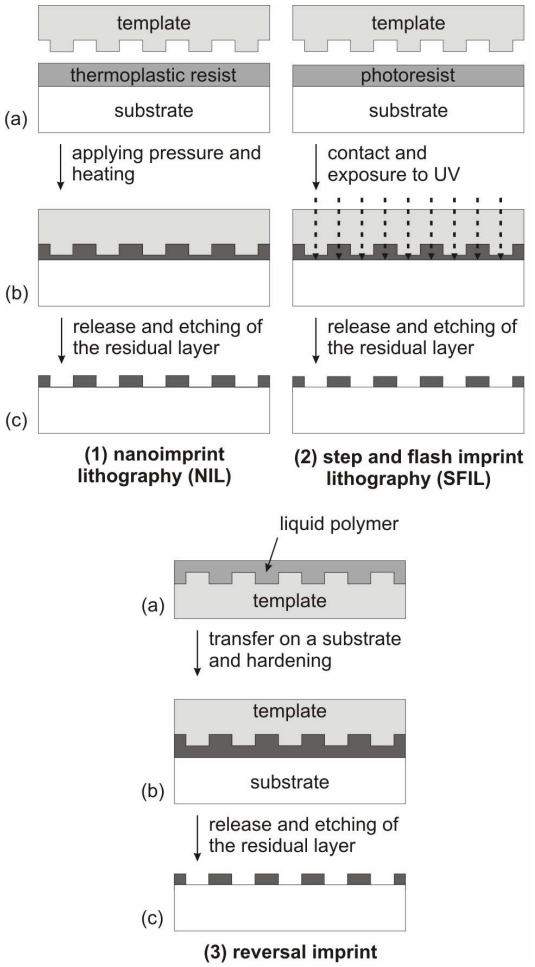

Figure 3. A few techniques to pattern polymers. (1) nanoimprint lithography (NIL): (a) a thermoplastic resist is spin-coated, (b) the plastic is heated above its glass temperature T_g and a template (fabricated using silicon technologies) is pressed against it, (c) the template is released and the residual layer etched using an oxygen plasma (71), (2) step-and-flash imprint lithography (SFIL): (a) a photoresist is deposited, (b) and exposed to UV while the template is pressed against it, (c) the template is released

and the residual layer etched using an oxygen plasma (72) and (3) reversal imprint: (a) a liquid polymer or prepolymer is spin-coated on the template, then (b) transferred on a substrate and hardened, (c) the template is released and the residual layer etched (73).

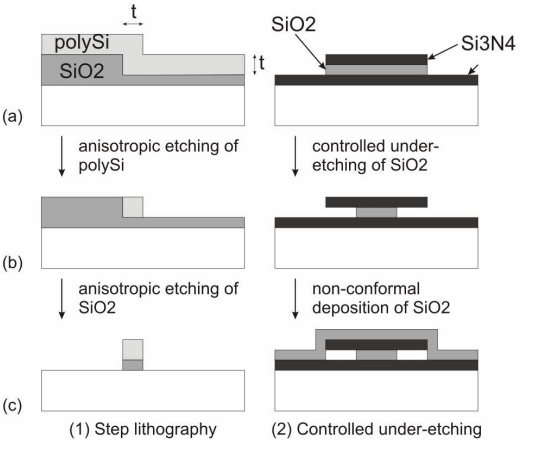

Figure 4. Two examples of edge lithography. (1) Step lithography: Starting from a layer of polySi deposited on a step etched in SiO_2(a), a selective and anisotropic etching is performed in the polySi (b), and next in the SiO_2 (127), (2) Controlled under-etching: starting from a stack of $Si_3N_4/SiO_2/Si_3N_4$ etched down the first Si_3N_4 layer (a), the SiO_2 layer is under-etched (b) and the channel is sealed by a non-conformal deposition (c) (122).

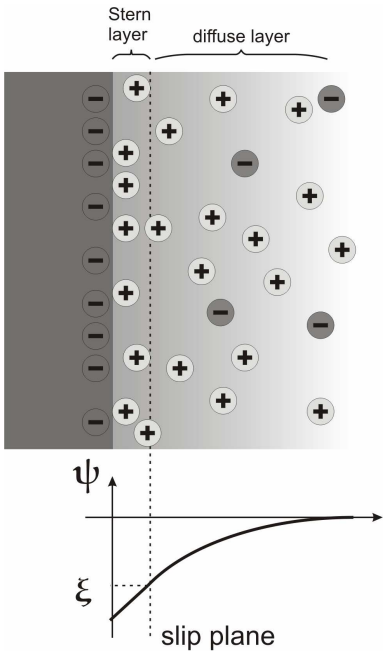

Figure 5. Schematic model of the electrical double layer at an interface solid/liquid. ψ is the electrical potential. A surface with negative charges is considered. These charges are shielded by the Stern layer and the diffuse layer. The Stern layer is formed by adsorbed immobile ions. The mobile diffuse layer is located outside the shear plane. The zeta potential ξ is at the shear plane. The Stern layer and the diffuse layer form the electrical double layer.

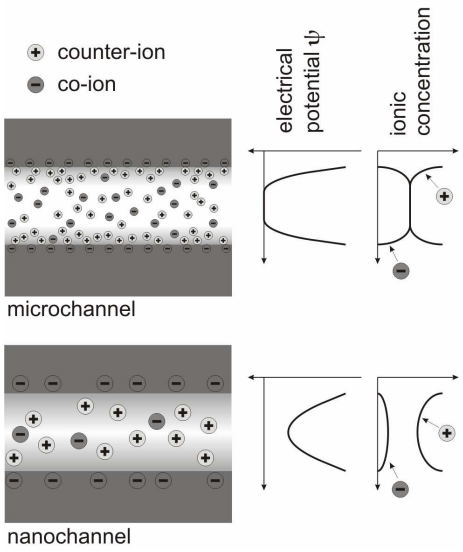

Figure 6. Illustration of differences in the electric potential and the ionic concentration in a microchannel and in a nanochannel. In a microchannel, the electrical double layer is much smaller than the typical dimensions. The potential is neutral in most of the channel. In a nanochannel, the Debye length is not negligible compared to the typical dimensions, leading to an excess of counterions in the electrolyte.

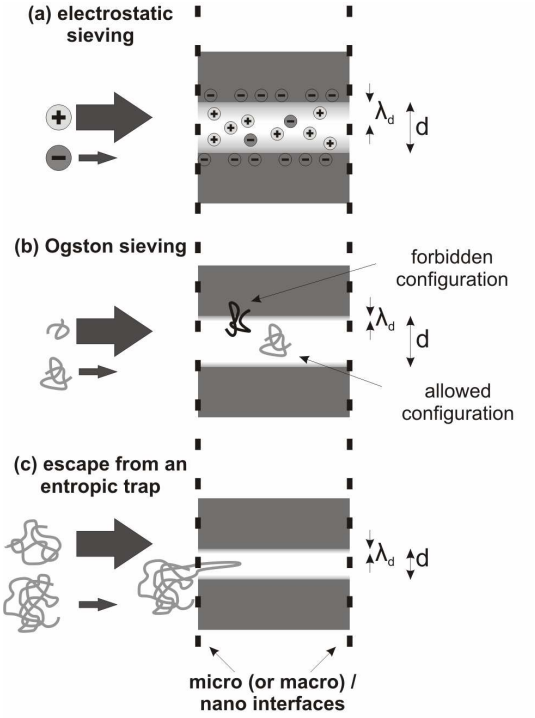

Figure 7. Schematics of some sieving mechanisms at the entrance of a circular nanochannel with a diameter *d*. The arrows on the left side of the figure symbolize the relative transport rates. Electrostatic sieving (a) is predominant when λ_d is similar to *d*. Counterions have a higher transport rate than coions. Steric and entropic effects become dominant when λ_d is negligible compared to *d*. Due to the confinement, chain-like molecules smaller than *d* have less orientational and conformational freedom resulting in a loss of entropy. Therefore smaller molecules have a higher transport rate (Ogston sieving, (b)). Molecules larger than *d* have to unfold to go through the channel, reducing their entropy (entropic trapping, (c)). The entropy barrier is larger for longer molecules leading to a lower transport rate. This is not true for a rectangular nanoslit (height < size of the molecule < width), where larger molecules have a

higher contact area with the entrance, so a higher probability to form a loop entering the channel, resulting in a higher transport rate.

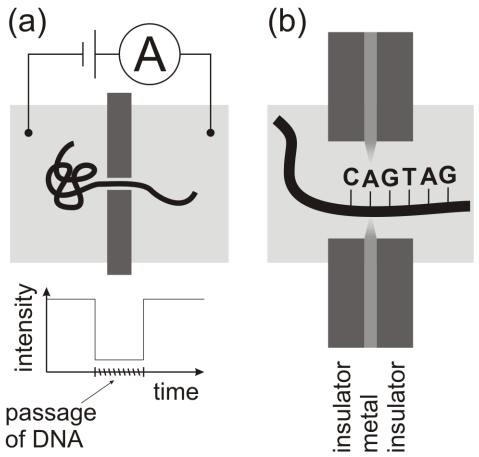

Figure 8. Scanning a single DNA molecule with a nanopore. (a) By applying a voltage, a DNA strand is stretched through the pore. The passage of the strand reduces the measured current during a certain time proportional to the length of DNA. (b) In the future, smart nanopores made through several layers may be able to read nucleotides one by one like a magnetic tape.

LITERATURE CITED

(1) Volkmuth, W. D.; Austin, R. H. *Nature* **1992**, *358*, 600-602.
(2) Gajar, S. A.; Geis, M. W. *Journal of the Electrochemical Society* **1992**, *139*, 2833-2840.
(3) Eijkel, J. C. T.; van den Berg, A. *Microfluidics and Nanofluidics* **2005**, *1*, 249-267.
(4) Yuan, Z.; Garcia, A. L.; Lopez, G. P.; Petsev, D. N. *Electrophoresis* **2007**, *28*, 595-610.
(5) Mijatovic, D.; Eijkel, J. C. T.; van den Berg, A. *Lab on a Chip* **2005**, *5*, 492-500.
(6) Perry, J. L.; Kandlikar, S. G. *Microfluidics and Nanofluidics* **2006**, *2*, 185-193.
(7) Mela, P.; Tas, N. R.; Berenschot, E. J. W.; van Nieuwkasteele, J.; van den Berg, A. *Electrophoresis* **2004**, *25*, 3687-3693.
(8) Pallandre, A.; de Lambert, B.; Attia, R.; Jonas, A. M.; Viovy, J. L. *Electrophoresis* **2006**, *27*, 584-610.
(9) Kumar, A.; Whitesides, G. M. *Applied Physics Letters* **1993**, *63*, 2002-2004.
(10) Hui, C. Y.; Jagota, A.; Lin, Y. Y.; Kramer, E. J. *Langmuir* **2002**, *18*, 1394-1407.
(11) Bhushan, B. *Journal of Vacuum Science & Technology B* **2003**, *21*, 2262-2296.
(12) Delrio, F. W.; De Boer, M. P.; Knapp, J. A.; Reedy, E. D.; Clews, P. J.; Dunn, M. L. *Nature Materials* **2005**, *4*, 629-634.
(13) Parker, E. E.; Ashurst, W. R.; Carraro, C.; Maboudian, R. *Journal of Microelectromechanical Systems* **2005**, *14*, 947-953.
(14) Han, J.; Craighead, H. G. *Journal of Vacuum Science & Technology A* **1999**, *17*, 2142-2147.

(15) Mao, P.; Han, J. Y. *Lab on a Chip* **2005**, *5*, 837-844.
(16) Kameoka, J.; Craighead, H. G. *Sensors and Actuators B-Chemical* **2001**, *77*, 632-637.
(17) Stein, D.; Kruithof, M.; Dekker, C. *Physical Review Letters* **2004**, *93*.
(18) Wang, H. Y.; Foote, R. S.; Jacobson, S. C.; Schneibel, J. H.; Ramsey, J. M. *Sensors and Actuators B-Chemical* **1997**, *45*, 199-207.
(19) Haneveld, J.; Jansen, H.; Berenschot, E.; Tas, N.; Elwenspoek, M. *Journal of Micromechanics and Microengineering* **2003**, *13*, S62-S66.
(20) Kutchoukov, V. G.; Laugere, F.; van der Vlist, W.; Pakula, L.; Garini, Y.; Bossche, A. *Sensors and Actuators a-Physical* **2004**, *114*, 521-527.
(21) Datta, A.; Choi, H. S.; Li, X. C. *Journal of the Electrochemical Society* **2006**, *153*, H89-H93.
(22) Schoch, R. B.; Renaud, P. *Applied Physics Letters* **2005**, *86*.
(23) Studer, V.; Pepin, A.; Chen, Y. *Applied Physics Letters* **2002**, *80*, 3614-3616.
(24) Abgrall, P.; Low, L. N.; Nguyen, N. T. *Lab on a Chip* **2007**, *7*, 520-522.
(25) Hu, W.; Yang, B.; Peng, C.; Pang, S. W. *Journal of Vacuum Science & Technology B* **2006**, *24*, 2225-2229.
(26) Yang, B.; Pang, S. W. *Journal of Vacuum Science & Technology B* **2006**, *24*, 2984-2987.
(27) Karnik, R.; Fan, R.; Yue, M.; Li, D. Y.; Yang, P. D.; Majumdar, A. *Nano Letters* **2005**, *5*, 943-948.
(28) Stern, M. B.; Geis, M. W.; Curtin, J. E. *Journal of Vacuum Science & Technology B* **1997**, *15*, 2887-2891.
(29) Tas, N. R.; Mela, P.; Kramer, T.; Berenschot, J. W.; van den Berg, A. *Nano Letters* **2003**, *3*, 1537-1540.
(30) Tas, N. R.; Berenschot, J. W.; Lammerink, T. S. J.; Elwenspoek, M.; van den Berg, A. *Analytical Chemistry* **2002**, *74*, 2224-2227.
(31) Foquet, M.; Korlach, J.; Zipfel, W.; Webb, W. W.; Craighead, H. G. *Analytical Chemistry* **2002**, *74*, 1415-1422.
(32) Eijkel, J. C. T.; Bomer, J.; Tas, N. R.; van den Berg, A. *Lab on a Chip* **2004**, *4*, 161-163.
(33) Nam, W. J.; Bae, S.; Kalkan, A. K.; Fonash, S. J. *Journal of Vacuum Science & Technology a-Vacuum Surfaces and Films* **2001**, *19*, 1229-1233.
(34) Cheng, G. J.; Pirzada, D.; Dutta, P. *Journal of Microlithography Microfabrication and Microsystems* **2005**, *4*, 013009.
(35) Zeng, H. J.; Wang, Z. L.; Feinerman, A. D. *Nanotechnology* **2006**, *17*, 3183-3188.
(36) Zevenbergen, M. A. G.; Krapf, D.; Zuiddam, M. R.; Lemay, S. G. *Nano Letters* **2007**, *7*, 384-388.
(37) Harnett, C. K.; Coates, G. W.; Craighead, H. G. *Journal of Vacuum Science & Technology B* **2001**, *19*, 2842-2845.
(38) Li, W. L.; Tegenfeldt, J. O.; Chen, L.; Austin, R. H.; Chou, S. Y.; Kohl, P. A.; Krotine, J.; Sturm, J. C. *Nanotechnology* **2003**, *14*, 578-583.
(39) ITRS, http://www.itrs.net/reports.html, 2005.
(40) Rothschild, M.; Bloomstein, T. M.; Efremow Jr., N.; Fedynyshyn, T. H.; Fritze, M.; Pottebaum, I.; Switkes, M. *MRS bulletin* **2005**, *30*, 942.
(41) Christensen, C. P.; Lakin, K. M. *Applied physics letters* **1978**, *32*, 254-256.
(42) Chin, B. H.; Ehrlich, G. *Applied Physics Letters* **1981**, *38*, 253-255.
(43) Melngailis, J. *Journal of Vacuum Science & Technology B* **1987**, *5*, 469-495.
(44) Yamasaki, K.; Juodkazis, S.; Matsuo, S.; Misawa, H. *Applied Physics a-Materials Science & Processing* **2003**, *77*, 371-373.
(45) Ke, K.; Hasselbrink, E. F.; Hunt, A. J. *Analytical Chemistry* **2005**, *77*, 5083-5088.
(46) Mullenborn, M.; Dirac, H.; Petersen, J. W. *Applied Physics Letters* **1995**, *66*, 3001-3003.
(47) Lercel, M. J.; Craighead, H. G.; Parikh, A. N.; Seshadri, K.; Allara, D. L. *Journal of Vacuum Science & Technology a-Vacuum Surfaces and Films* **1996**, *14*, 1844-1849.
(48) Yasin, S.; Hasko, D. G.; Ahmed, H. *Applied Physics Letters* **2001**, *78*, 2760-2762.

(49) Reccius, C. H.; Mannion, J. T.; Cross, J. D.; Craighead, H. G. *Physical Review Letters* **2005**, *95*.
(50) Hibara, A.; Saito, T.; Kim, H. B.; Tokeshi, M.; Ooi, T.; Nakao, M.; Kitamori, T. *Analytical Chemistry* **2002**, *74*, 6170-6176.
(51) Riehn, R.; Austin, R. H. *Analytical Chemistry* **2006**, *78*, 5933-5934.
(52) Peng, C. Y.; Nam, W. J.; Fonash, S. J.; Gu, B.; Sen, A.; Strawhecker, K.; Natarajan, S.; Foley, H. C.; Kim, S. H. *Journal of the American Chemical Society* **2003**, *125*, 9298-9299.
(53) Turner, S. W.; Perez, A. M.; Lopez, A.; Craighead, H. *Journal of Vacuum Science & Technology B* **1998**, *16*, 3835-3840.
(54) Jayachandran, J. P.; Kelleher, H. A.; Allen, S. A. B.; Kohl, P. A. *Journal of Micromechanics and Microengineering* **2005**, *15*, 35-42.
(55) Campbell, L. C.; Wilkinson, M. J.; Manz, A.; Camilleri, P.; Humphreys, C. J. *Lab on a Chip* **2004**, *4*, 225-229.
(56) Arscott, S.; Troadec, D. *Nanotechnology* **2005**, *16*, 2295-2302.
(57) Mahabadi, K. A.; Rodriguez, I.; Haur, S. C.; van Kan, J. A.; Bettiol, A. A.; Watt, F. *Journal of Micromechanics and Microengineering* **2006**, *16*, 1170-1180.
(58) Kramer, S.; Fuierer, R. R.; Gorman, C. B. *Chemical Reviews* **2003**, *103*, 4367-4418.
(59) Geissler, M.; Xia, Y. N. *Advanced Materials* **2004**, *16*, 1249-1269.
(60) Ginger, D. S.; Zhang, H.; Mirkin, C. A. *Angewandte Chemie-International Edition* **2004**, *43*, 30-45.
(61) Gates, B. D.; Xu, Q. B.; Stewart, M.; Ryan, D.; Willson, C. G.; Whitesides, G. M. *Chemical Reviews* **2005**, *105*, 1171-1196.
(62) Eigler, D. M.; Schweizer, E. K. *Nature* **1990**, *344*, 524-526.
(63) Piner, R. D.; Zhu, J.; Xu, F.; Hong, S. H.; Mirkin, C. A. *Science* **1999**, *283*, 661-663.
(64) Liu, G. Y.; Xu, S.; Qian, Y. L. *Accounts of Chemical Research* **2000**, *33*, 457-466.
(65) Dai, H. J.; Franklin, N.; Han, J. *Applied Physics Letters* **1998**, *73*, 1508-1510.
(66) Vettiger, P.; Brugger, J.; Despont, M.; Drechsler, U.; Durig, U.; Haberle, W.; Lutwyche, M.; Rothuizen, H.; Stutz, R.; Widmer, R.; Binnig, G. *Microelectronic Engineering* **1999**, *46*, 11-17.
(67) Harfenist, S. A.; Cambron, S. D.; Nelson, E. W.; Berry, S. M.; Isham, A. W.; Crain, M. M.; Walsh, K. M.; Keynton, R. S.; Cohn, R. W. *Nanolett.* **2004**, *4*, 1931-1937.
(68) McCord, M. A. *Journal of Vacuum Science & Technology B* **1997**, *15*, 2125-2129.
(69) Heckele, M.; Schomburg, W. K. *Journal of Micromechanics and Microengineering* **2004**, *14*, R1-R14.
(70) Guo, L. J. *Advanced Materials* **2007**, *19*, 495-513.
(71) Chou, S. Y.; Krauss, P. R.; Renstrom, P. J. *Applied Physics Letters* **1995**, *67*, 3114-3116.
(72) Ruchhoeft, P.; Colburn, M.; Choi, B.; Nounu, H.; Johnson, S.; Bailey, T.; Damle, S.; Stewart, M.; Ekerdt, J.; Sreenivasan, S. V.; Wolfe, J. C.; Willson, C. G. *Journal of Vacuum Science & Technology B* **1999**, *17*, 2965-2969.
(73) Huang, X. D.; Bao, L. R.; Cheng, X.; Guo, L. J.; Pang, S. W.; Yee, A. F. *Journal of Vacuum Science & Technology B* **2002**, *20*, 2872-2876.
(74) Borzenko, T.; Tormen, M.; Schmidt, G.; Molenkamp, L. W.; Janssen, H. *Applied Physics Letters* **2001**, *79*, 2246-2248.
(75) Zhao, X. M.; Xia, Y. N.; Whitesides, G. M. *Advanced Materials* **1996**, *8*, 837-840.
(76) Loo, Y. L.; Hsu, J. W. P.; Willett, R. L.; Baldwin, K. W.; West, K. W.; Rogers, J. A. *Journal of Vacuum Science & Technology B* **2002**, *20*, 2853-2856.
(77) Kim, E.; Xia, Y. N.; Zhao, X. M.; Whitesides, G. M. *Advanced Materials* **1997**, *9*, 651-654.
(78) Tegenfeldt, J. O.; Prinz, C.; Cao, H.; Chou, S.; Reisner, W. W.; Riehn, R.; Wang, Y. M.; Cox, E. C.; Sturm, J. C.; Silberzan, P.; Austin, R. H. *Proceedings of the National Academy of Sciences of the United States of America* **2004**, *101*, 10979-10983.
(79) Reisner, W.; Morton, K. J.; Riehn, R.; Wang, Y. M.; Yu, Z. N.; Rosen, M.; Sturm, J. C.; Chou, S. Y.; Frey, E.; Austin, R. H. *Physical Review Letters* **2005**, *94*.
(80) Reano, R. M.; Pang, S. W. *Journal of Vacuum Science & Technology B* **2005**, *23*, 2995-2999.

(81) Cao, H.; Yu, Z. N.; Wang, J.; Tegenfeldt, J. O.; Austin, R. H.; Chen, E.; Wu, W.; Chou, S. Y. *Applied Physics Letters* **2002**, *81*, 174-176.
(82) Guo, L. J.; Cheng, X.; Chou, C. F. *Nano Letters* **2004**, *4*, 69-73.
(83) Saleh, O. A.; Sohn, L. L. *Nanoletters* **2003**, *3*, 37-38.
(84) Erickson, D.; Rockwood, T.; Emery, T.; Scherer, A.; Psaltis, D. *Optics Letters* **2006**, *31*, 59-61.
(85) Schmid, H.; Michel, B. *Macromolecules* **2000**, *33*, 3042-3049.
(86) Odom, T. W.; Love, J. C.; Wolfe, D. B.; Paul, K. E.; Whitesides, G. M. *Langmuir* **2002**, *18*, 5314-5320.
(87) Huh, D.; Mills, K. L.; Zhu, X.; Burns, M. A.; Thouless, M. D.; Takayama, S. *Nature Materials* **2007**, *6*, 424-428.
(88) Bowden, N.; Huck, W. T. S.; Paul, K. E.; Whitesides, G. M. *Applied Physics Letters* **1999**, *75*, 2557-2559.
(89) Truong, T. Q.; Nguyen, N. T. *Journal of Micromechanics and Microengineering* **2004**, *14*, 632-638.
(90) Abgrall, P.; Lattes, C.; Conedera, V.; Dollat, X.; Colin, S.; Gue, A. M. *Journal of Micromechanics and Microengineering* **2006**, *16*, 113-121.
(91) Unger, M. A.; Chou, H. P.; Thorsen, T.; Scherer, A.; Quake, S. R. *Science* **2000**, *288*, 113-116.
(92) Zaumseil, J.; Meitl, M. A.; Hsu, J. W. P.; Acharya, B. R.; Baldwin, K. W.; Loo, Y. L.; Rogers, J. A. *Nano Letters* **2003**, *3*, 1223-1227.
(93) Jeon, S.; Menard, E.; Park, J. U.; Maria, J.; Meitl, M.; Zaumseil, J.; Rogers, J. A. *Advanced Materials* **2004**, *16*, 1369-1373.
(94) Dumond, J. J.; Low, H. Y.; Rodriguez, I. *Nanotechnology* **2006**, *17*, 1975-1980.
(95) Nakajima, M.; Yoshikawa, T.; Sogo, K.; Hirai, Y. *Microelectronic Engineering* **2006**, *83*, 876-879.
(96) Kim, P.; Jeong, H. E.; Khademhosseini, A.; Suh, K. Y. *Lab on a Chip* **2006**, *6*, 1432-1437.
(97) Seemann, R.; Kramer, E. J.; Lange, F. F. *New Journal of Physics* **2004**, *6*.
(98) Register, R. A. *Nature* **2003**, *424*, 378-379.
(99) Segalman, R. A. *Materials Science & Engineering R-Reports* **2005**, *48*, 191-226.
(100) Rzayev, J.; Hillmyer, M. A. *Journal of the American Chemical Society* **2005**, *127*, 13373-13379.
(101) Gogotsi, Y.; Libera, J. A.; Guvenc-Yazicioglu, A.; Megaridis, C. M. *Applied Physics Letters* **2001**, *79*, 1021-1023.
(102) Melechko, A. V.; McKnight, T. E.; Guillorn, M. A.; Merkulov, V. I.; Ilic, B.; Doktycz, M. J.; Lowndes, D. H.; Simpson, M. L. *Applied Physics Letters* **2003**, *82*, 976-978.
(103) Wang, Z. K.; Ci, L. J.; Chen, L.; Nayak, S.; Ajayan, P. M.; Koratkar, N. *Nano Letters* **2007**, *7*, 697-702.
(104) Holt, J. K.; Park, H. G.; Wang, Y. M.; Stadermann, M.; Artyukhin, A. B.; Grigoropoulos, C. P.; Noy, A.; Bakajin, O. *Science* **2006**, *312*, 1034-1037.
(105) Chen, J. Y.; Kutana, A.; Collier, C. P.; Giapis, K. P. *Science* **2005**, *310*, 1480-1483.
(106) Hinds, B. J.; Chopra, N.; Rantell, T.; Andrews, R.; Gavalas, V.; Bachas, L. G. *Science* **2007**, *303*, 62-65.
(107) Riegelman, M.; Liu, H.; Bau, H. H. *Journal of Fluids Engineering-Transactions of the Asme* **2006**, *128*, 6-13.
(108) Sivanesan, P.; Okamoto, K.; English, D.; Lee, C. S.; DeVoe, D. L. *Analytical Chemistry* **2005**, *77*, 2252-2258.
(109) Czaplewski, D. A.; Kameoka, J.; Mathers, R.; Coates, G. W.; Craighead, H. G. *Applied Physics Letters* **2003**, *83*, 4836-4838.
(110) Verbridge, S. S.; Edel, J. B.; Stavis, S. M.; Moran-Mirabal, J. M.; Allen, S. D.; Coates, G.; Craighead, H. G. *Journal of Applied Physics* **2005**, *97*.
(111) Wang, M.; Jing, N.; Su, C. B.; Kameoka, J.; Chou, C. K.; Hung, M. C.; Chang, K. A. *Applied Physics Letters* **2006**, *88*.
(112) Evans, E.; Bowman, H.; Leung, A.; Needham, D.; Tirrel, D. *Science* **1996**, *273*, 933-935.

(113) Karlsson, A.; Karlsson, R.; Karlsson, M.; Cans, A. S.; Stromberg, A.; Ryttsen, F.; Orwar, O. *Nature* **2001**, *409*, 150-152.
(114) Karlsson, M.; Sott, K.; Davidson, M.; Cans, A. S.; Linderholm, P.; Chiu, D.; Orwar, O. *Proceedings of the National Academy of Sciences of the United States of America* **2002**, *99*, 11573-11578.
(115) Lobovkina, T.; Dommersnes, P.; Joanny, J. F.; Bassereau, P.; Karlsson, M.; Orwar, O. *Proceedings of the National Academy of Sciences of the United States of America* **2004**, *101*, 7949-7953.
(116) Karlsson, R.; Karlsson, M.; Karlsson, A.; Cans, A. S.; Bergenholtz, J.; Akerman, B.; Ewing, A. G.; Voinova, M.; Orwar, O. *Langmuir* **2002**, *18*, 4186-4190.
(117) Karlsson, R.; Karlsson, A.; Orwar, O. *Journal of Physical Chemistry B* **2003**, *107*, 11201-11207.
(118) Tokarz, M.; Akerman, B.; Olofsson, J.; Joanny, J. F.; Dommersnes, P.; Orwar, O. *Proceedings of the National Academy of Sciences of the United States of America* **2005**, *102*, 9127-9132.
(119) Reiner, J. E.; Wells, J. M.; Kishore, R. B.; Pfefferkorn, C.; Helmerson, K. *Proceedings of the National Academy of Sciences of the United States of America* **2006**, *103*, 1173-1177.
(120) Harfenist, S. A.; Cambron, S. D.; Nelson, E. W.; Berry, S. M.; Isham, A. W.; Crain, M. M.; Walsh, K. M.; Keynton, R. S.; Cohn, R. W. *Nano Letters* **2004**, *4*, 1931-1937.
(121) Pearson, J. L.; Cumming, D. R. S. *Journal of Vacuum Science & Technology B* **2005**, *23*, 2793-2797.
(122) Han, A. P.; de Rooij, N. F.; Staufer, U. *Nanotechnology* **2006**, *17*, 2498-2503.
(123) Lee, C.; Yang, E. H.; Myung, N. V.; George, T. *Nano Letters* **2003**, *3*, 1339-1340.
(124) Ilic, B.; Czaplewski, D.; Zalalutdinov, M.; Schmidt, B.; Craighead, H. G. *Journal of Vacuum Science & Technology B* **2002**, *20*, 2459-2465.
(125) Chen, X.; Ji, R.; Steinhart, M.; Milenin, A.; Nielsch, K.; Gosele, U. *Chemistry of Materials* **2007**, *19*, 3-5.
(126) Hug, T. S.; de Rooij, N. F.; Staufer, U. *Microfluidics and Nanofluidics* **2006**, *2*, 117-124.
(127) Fu, H. S.; US4358340A1, Ed.: USA, 1980; Vol. US4358340A1.
(128) Tas, N. R.; Berenschot, J. W.; Mela, P.; Jansen, H. V.; Elwenspoek, M.; van den Berg, A. *Nano Letters* **2002**, *2*, 1031-1032.
(129) Love, J. C.; Paul, K. E.; Whitesides, G. M. *Advanced Materials* **2001**, *13*, 604-+.
(130) Fritze, M.; Tyrell, B. M.; Astolfi, D. K.; Lambert, R. D.; Yost, D. R. W.; Forte, A. R.; Cann, S. G.; Wheeler, B. D. *Lincoln Laboratory Journal* **2003**, *14*.
(131) Rogers, J. A.; Paul, K. E.; Jackman, R. J.; Whitesides, G. M. *Applied Physics Letters* **1997**, *70*, 2658-2660.
(132) Odom, T. W.; Thalladi, V. R.; Love, J. C.; Whitesides, G. M. *Journal of the American Chemical Society* **2002**, *124*, 12112-12113.
(133) Rogers, J. A.; Paul, K. E.; Jackman, R. J.; Whitesides, G. M. *Journal of Vacuum Science & Technology B* **1998**, *16*, 59-68.
(134) Jeon, S.; Malyarchuk, V.; White, J. O.; Rogers, J. A. *Nano Letters* **2005**, *5*, 1351-1356.
(135) Brueck, S. R. J. *Proceedings of the Ieee* **2005**, *93*, 1704-1721.
(136) O'Brien, M. J.; Bisong, P.; Ista, L. K.; Rabinovich, E. M.; Garcia, A. L.; Sibbett, S. S.; Lopez, G. P.; Brueck, S. R. J. *Journal of Vacuum Science & Technology B* **2003**, *21*, 2941-2945.
(137) Jang, J. H.; Ullal, C. K.; Gorishnyy, T.; Tsukruk, V. V.; Thomas, E. L. *Nano Letters* **2006**, *6*, 740-743.
(138) Garcia, A. L.; Ista, L. K.; Petsev, D. N.; O'Brien, M. J.; Bisong, P.; Mammoli, A. A.; Brueck, S. R. J.; Lopez, G. P. *Lab on a Chip* **2005**, *5*, 1271-1276.
(139) Ayazi, F.; Najafi, K. *Sensors and Actuators a-Physical* **2000**, *87*, 46-51.
(140) Pourkamali, S.; Hashimura, A.; Abdolvand, R.; Ho, G. K.; Erbil, A.; Ayazi, F. *Journal of Microelectromechanical Systems* **2003**, *12*, 487-496.
(141) Martin, F.; Walczak, R.; Boiarski, A.; Cohen, M.; West, T.; Cosentino, C.; Shapiro, J.; Ferrari, M. *Journal of Controlled Release* **2005**, *107*, 183-183.

(142) Kim, H. C.; Kim, D. H.; Chun, K. *Journal of Micromechanics and Microengineering* **2006**, *16*, 906-913.
(143) Weigold, J. W.; Najafi, K.; Pang, S. W. *Journal of Microelectromechanical Systems* **2001**, *10*, 518-524.
(144) Pourkamali, S.; Ayazi, F. In *Mems 2004: 17th Ieee International Conference on Micro Electro Mechanical Systems, Technical Digest*, 2004, pp 813-816.
(145) Kwon, S. J.; Jeong, Y. M.; Jeong, S. H. *Applied Physics a-Materials Science & Processing* **2007**, *86*, 11-18.
(146) Dekker, C. *Nature Nanotechnology* **2007**, *2*, 209-215.
(147) Kasianowicz, J. J.; Brandin, E.; Branton, D.; Deamer, D. W. *Proceedings of the National Academy of Sciences of the United States of America* **1996**, *93*, 13770-13773.
(148) Siwy, Z.; Fulinski, A. *Physical Review Letters* **2002**, *89*.
(149) Li, J.; Stein, D.; McMullan, C.; Branton, D.; Aziz, M. J.; Golovchenko, J. A. *Nature* **2001**, *412*, 166-169.
(150) Storm, A. J.; Chen, J. H.; Ling, X. S.; Zandbergen, H. W.; Dekker, C. *Nature Materials* **2003**, *2*, 537-540.
(151) Krapf, D.; Wu, M. Y.; Smeets, R. M. M.; Zandbergen, H. W.; Dekker, C.; Lemay, S. G. *Nano Letters* **2006**, *6*, 105-109.
(152) Kirby, B. J.; Hasselbrink, E. F. *Electrophoresis* **2004**, *25*, 187-202.
(153) de Jong, J.; Lammertink, R. G. H.; Wessling, M. *Lab on a Chip* **2006**, *6*, 1125-1139.
(154) Karnik, R.; Castelino, K.; Fan, R.; Yang, P.; Majumdar, A. *Nano Letters* **2005**, *5*, 1638-1642.
(155) Schoch, R. B.; van Lintel, H.; Renaud, P. *Physics of Fluids* **2005**, *17*.
(156) Fan, R.; Yue, M.; Karnik, R.; Majumdar, A.; Yang, P. D. *Physical Review Letters* **2005**, *95*.
(157) Plecis, A.; Schoch, R. B.; Renaud, P. *Nano Letters* **2005**, *5*, 1147-1155.
(158) Pu, Q. S.; Yun, J. S.; Temkin, H.; Liu, S. R. *Nano Letters* **2004**, *4*, 1099-1103.
(159) Conlisk, A. T.; McFerran, J.; Zheng, Z.; Hansford, D. *Analytical Chemistry* **2002**, *74*, 2139-2150.
(160) Conlisk, A. T. *Electrophoresis* **2005**, *26*, 1896-1912.
(161) De Leebeeck, A.; Sinton, D. *Electrophoresis* **2006**, *27*, 4999-5008.
(162) Huang, K. D.; Yang, R. J. *Nanotechnology* **2007**, *18*.
(163) Taylor, J.; Ren, C. L. *Microfluidics and Nanofluidics* **2005**, *1*, 356-363.
(164) Burgreen, D.; Nakache, F. R. *Journal of physical chemistry* **1963**, *68*, 1084-1091.
(165) Pennathur, S.; Santiago, J. G. *Analytical Chemistry* **2005**, *77*, 6772-6781.
(166) van der Heyden, F. H. J.; Stein, D.; Dekker, C. *Physical Review Letters* **2005**, *95*.
(167) Qiao, R.; Aluru, N. R. *Nano Letters* **2003**, *3*, 1013-1017.
(168) Qiao, R.; Aluru, N. R. *Journal of Chemical Physics* **2003**, *118*, 4692-4701.
(169) Qiao, R.; Aluru, N. R. *Physical Review Letters* **2004**, *92*.
(170) Qiao, R.; Aluru, N. R. *Colloids and Surfaces a-Physicochemical and Engineering Aspects* **2005**, *267*, 103-109.
(171) Qiao, R.; Aluru, N. R. *Langmuir* **2005**, *21*, 8972-8977.
(172) Washburn, E. W. *Physical Review* **1921**, *17*, 273-283.
(173) Sobolev, V. D.; Churaev, N. V.; Velarde, M. G.; Zorin, Z. M. *Journal of colloid and interface science* **2000**, *222*, 51-54.
(174) Tas, N. R.; Haneveld, J.; Jansen, H. V.; Elwenspoek, M.; van den Berg, A. *Applied Physics Letters* **2004**, *85*, 3274-3276.
(175) Han, A.; Mondin, G.; Hegelbach, N. G.; de Rooij, N. F.; Staufer, U. *Journal of Colloid and Interface Science* **2006**, *293*, 151-157.
(176) van Delft, K. M.; Eijkel, J. C. T.; Mijatovic, D.; Druzhinina, T. S.; Rathgen, H.; Tas, N. R.; van den Berg, A.; Mugele, F. *Nano Letters* **2007**, *7*, 345-350.
(177) Kaji, N.; Ogawa, R.; Oki, A.; Horiike, Y.; Tokeshi, M.; Baba, Y. *Analytical and Bioanalytical Chemistry* **2006**, *386*, 759-764.

(178) Eijkel, J. C. T.; Dan, B.; Reemeijer, H. W.; Hermes, D. C.; Bomer, J. G.; van den Berg, A. *Physical Review Letters* **2005**, *95*.
(179) van Honschoten, J. W.; Escalante, M.; Tas, N. R.; Jansen, H. V.; Elwenspoek, M. *Journal of Applied Physics* **2007**, *101*.
(180) Vinogradova, O. I. *International Journal of Mineral Processing* **1999**, *56*, 31-60.
(181) Eijkel, J. *Lab on a Chip* **2007**, *7*, 299-301.
(182) Joseph, P.; Cottin-Bizonne, C.; Benoit, J. M.; Ybert, C.; Journet, C.; Tabeling, P.; Bocquet, L. *Physical review letters* **2006**, *97*, 156104.
(183) Joly, L.; Ybert, C.; Trizac, E.; Bocquet, L. *Physical Review Letters* **2004**, *93*.
(184) Joly, L.; Ybert, C.; Trizac, E.; Bocquet, L. *Journal of Chemical Physics* **2006**, *125*.
(185) Majumder, M.; Chopra, N.; Andrews, R.; Hinds, B. J. *Nature* **2005**, *438*, 44.
(186) Holt, J. K.; Park, H. G.; Wang, Y.; Stadermann, M.; Artyukhin, A. B.; Grigoropoulos, C. P.; Noy, A.; Bakajin, O. *Science* **2006**, *312*, 1034-1037.
(187) Tegenfeldt, J. O.; Prinz, C.; Cao, H.; Huang, R. L.; Austin, R. H.; Chou, S. Y.; Cox, E. C.; Sturm, J. C. *Analytical and Bioanalytical Chemistry* **2004**, *378*, 1678-1692.
(188) Mohamadi, M. R.; Mahmoudian, L.; Kaji, N.; Tokeshi, M.; Chuman, H.; Baba, Y. *Nanotoday* **2006**, *1*, 38-45.
(189) Frantisek, S. *Journal of separation science* **2002**, *26*, 751-752.
(190) Viovy, J. L. *Review of modern physics* **2000**, *72*, 813-872.
(191) Slater, G. W.; Guillouzic, S.; Gauthier, M. G.; Mercier, J. F.; Kenward, M.; McCormick, L. C.; Tessier, F. *Electrophoresis* **2002**, *23*, 3791-3816.
(192) Eijkel, J. *Lab on a Chip* **2006**, *6*, 19-23.
(193) Fu, J. P.; Schoch, R. B.; Stevens, A. L.; Tannenbaum, S. R.; Han, J. Y. *Nature Nanotechnology* **2007**, *2*, 121-128.
(194) Arvanitidiou, E.; Hoagland, D. *Physical review letters* **1991**, *67*, 1464-1466.
(195) Rousseau, J.; Drouin, G.; Slater, G. W. *Physical review letters* **1997**, *79*, 1945-1948.
(196) Han, J.; Turner, S. W.; Craighead, H. G. *Physical Review Letters* **1999**, *83*, 1688-1691.
(197) Kuo, T. C.; Cannon, D. M.; Chen, Y. N.; Tulock, J. J.; Shannon, M. A.; Sweedler, J. V.; Bohn, P. W. *Analytical Chemistry* **2003**, *75*, 1861-1867.
(198) Chang, I. H.; Tulock, J. J.; Liu, J. W.; Kim, W. S.; Cannon, D. M.; Lu, Y.; Bohn, P. W.; Sweedler, J. V.; Cropek, D. M. *Environmental Science & Technology* **2005**, *39*, 3756-3761.
(199) Kirk, J. S.; Sweedler, J. V.; Bohn, P. W. *Analytical Chemistry* **2006**, *78*, 2335-2341.
(200) Schoch, R. B.; Bertsch, A.; Renaud, P. *Nano Letters* **2006**, *6*, 543-547.
(201) Durand, N. F. Y.; Bertsch, A.; Todorova, M.; Renaud, P. *Applied Physics Letters* **2007**, *91*.
(202) Karnik, R.; Castelino, K.; Majumdar, A. *Applied Physics Letters* **2006**, *88*.
(203) Khandurina, J.; Jacobson, S. C.; Waters, L. C.; Foote, R. S.; Ramsey, J. M. *Analytical chemistry* **1999**, *71*, 1815-1819.
(204) Bakajin, O.; Duke, T. A. J.; Tegenfeldt, J.; Chou, C. F.; Chan, S. C.; Austin, R. H.; Cox, E. C. *Analytical Chemistry* **2001**, *73*, 6053-6058.
(205) Zhang, Y.; Timperman, A. T. *Analyst* **2003**, *128*, 537-542.
(206) Wang, Y. C.; Stevens, A. L.; Han, J. Y. *Analytical Chemistry* **2005**, *77*, 4293-4299.
(207) Wang, Y. C.; Liu, V. H.; Han, J., The 11th International Conference on Miniaturized Systems for Chemistry and Life Sciences, MicroTAS, Paris 2007.
(208) Bakajin, O.; Duke, T. A. J.; Tegenfeldt, J.; Chou, C. F.; Chan, S. S.; Austin, R. H.; Cox, E. C. *Analytical Chemistry* **2001**, *73*, 6053-6056.
(209) Schwartz, D. C.; Cantor, C. R. *Cell* **1984**, *37*, 67-75.
(210) Sudor, J.; Novotny, M. *Proceedings of the National Academy of Sciences of the United States of America* **1993**, *90*, 9451-9455.
(211) Sudor, J.; Novotny, M. V. *Analytical Chemistry* **1994**, *66*, 2446-2450.
(212) Isambert, H.; Ajdari, A.; Viovy, J. L.; Prost, J. *Physical Review Letters* **1997**, *78*, 971-974.
(213) Stellwagen, N. C.; Gelfi, C.; Righetti, P. G. *Biopolymers* **1997**, *42*, 687-703.

(214) Cross, J. D.; Strychalski, E. A.; Craighead, H. G. *Journal of Applied Physics* **2007**, *102*.
(215) Pennathur, S.; Baldessari, F.; Santiago, J. G.; Kattah, M. G.; Steinman, J. B.; Utz, P. J. *Analytical Chemistry* **2007**, *79*, 8316-8322.
(216) Pennathur, S.; Santiago, J. G. *Analytical Chemistry* **2005**, *77*, 6782-6789.
(217) Clicq, D.; Vervoort, N.; Vounckx, R.; Ottevaere, H.; Buijs, J.; Gooijer, C.; Ariese, F.; Baron, G. V.; Desmet, G. *Journal of Chromatography A* **2002**, *979*, 33-42.
(218) Clicq, D.; Vankrunkelsven, S.; Ranson, W.; De Tandt, C.; Barn, G. V.; Desmet, G. *Analytica Chimica Acta* **2004**, *507*, 79-86.
(219) Han, J.; Craighead, H. G. *Science* **2000**, *288*, 1026-1029.
(220) Fu, J.; Mao, P.; Han, J. *Applied Physics Letters* **2005**, *87*, 263902.
(221) Fu, J. P.; Yoo, J.; Han, J. Y. *Physical Review Letters* **2006**, *97*.
(222) Baba, M.; Sano, T.; Iguchi, N.; Iida, K.; Sakamoto, T.; Kawaura, H. *Applied Physics Letters* **2003**, *83*, 1468-1470.
(223) He, B.; Tait, N.; Regnier, F. *Analytical Chemistry* **1998**, *70*, 3790-3797.
(224) Yin, N. F.; Killeen, K.; Brennen, R.; Sobek, D.; Werlich, M.; van de Goor, T. V. *Analytical Chemistry* **2005**, *77*, 527-533.
(225) Pamme, N. *Lab on a Chip* **2007**, *7*, 1644-1659.
(226) Raymond, D. E.; Manz, A.; Widmer, H. M. *Analytical Chemistry* **1994**, *66*, 2858-2865.
(227) Macounova, K.; Cabrera, C. R.; Yager, P. *Analytical Chemistry* **2001**, *73*, 1627-1633.
(228) Duke, T. A. J.; Austin, R. H. *Physical Review Letters* **1998**, *80*, 1552-1555.
(229) Chou, C. F.; Bakajin, O.; Turner, S. W. P.; Duke, T. A. J.; Chan, S. S.; Cox, E. C.; Craighead, H. G.; Austin, R. H. *Proceedings of the National Academy of Sciences of the United States of America* **1999**, *96*, 13762-13765.
(230) Huang, L. R.; Silberzan, P.; Tegenfeldt, J. O.; Cox, E. C.; Sturm, J. C.; Austin, R. H.; Craighead, H. *Physical Review Letters* **2002**, *89*.
(231) Cabodi, M.; Chen, Y. F.; Turner, S. W. P.; Craighead, H. G.; Austin, R. H. *Electrophoresis* **2002**, *23*, 3496-3503.
(232) Huang, L. R.; Tegenfeldt, J. O.; Kraeft, J. J.; Sturm, J. C.; Austin, R. H.; Cox, E. C. *Nature Biotechnology* **2002**, *20*, 1048-1051.
(233) Hattori, W.; Someya, H.; Baba, M.; Kawaura, H. *Journal of Chromatography A* **2004**, *1051*, 141-146.
(234) Huang, L. R.; Cox, E. C.; Austin, R. H.; Sturm, J. C. *Science* **2004**, *304*, 987-990.
(235) Mannion, J. T.; Craighead, H. G. *Biopolymers* **2007**, *85*, 131-143.
(236) Foquet, M.; Korlach, J.; Zipfel, W. R.; Webb, W. W.; Craighead, H. G. *Analytical Chemistry* **2004**, *76*, 1618-1626.
(237) Turner, S. W. P.; Cabodi, M.; Craighead, H. G. *Physical Review Letters* **2002**, *88*.
(238) Mannion, J. T.; Reccius, C. H.; Cross, J. D.; Craighead, H. G. *Biophysical Journal* **2006**, *90*, 4538-4545.
(239) Balducci, A.; Mao, P.; Han, J. Y.; Doyle, P. S. *Macromolecules* **2006**, *39*, 6273-6281.
(240) Riehn, R.; Austin, R. H.; Sturm, J. C. *Nano Letters* **2006**, *6*, 1973-1976.
(241) Tegenfeldt, J. O.; Cao, H.; Reisner, W. W.; Prinz, C.; Austin, R. H.; Chou, S. Y.; Cox, E. C.; Sturm, J. C. *Biophysical Journal* **2004**, *86*, 596A-596A.
(242) Wang, Y. M.; Tegenfeldt, J. O.; Reisner, W.; Riehn, R.; Guan, X. J.; Guo, L.; Golding, I.; Cox, E. C.; Sturm, J.; Austin, R. H. *Proceedings of the National Academy of Sciences of the United States of America* **2005**, *102*, 9796-9801.
(243) Jo, K.; Dhingra, D. M.; Odijk, T.; de Pablo, J. J.; Graham, M. D.; Runnheim, R.; Forrest, D.; Schwartz, D. C. *Proceedings of the National Academy of Sciences of the United States of America* **2007**, *104*, 2673-2678.
(244) Krishnan, M.; Monch, I.; Schwille, P. *Nano Letters* **2007**, *7*, 1270-1275.
(245) Reisner, W.; Beech, J. P.; Larsen, N. B.; Flyvbjerg, H.; Kristensen, A.; Tegenfeldt, J. O. *Physical Review Letters* **2007**, *99*.

(246) Stavis, S. M.; Edel, J. B.; Samiee, K. T.; Craighead, H. G. *Lab on a Chip* **2005**, *5*, 337-343.
(247) Fu, C. C.; Lee, H. Y.; Chen, K.; Lim, T. S.; Wu, H. Y.; Lin, P. K.; Wei, P. K.; Tsao, P. H.; Chang, H. C.; Fann, W. *PNAS* **2007**, *104*, 727-732.
(248) Deamer, D. W.; Aleson, M. *Trends in biotechnology* **2000**, *18*, 147-151.
(249) Fan, R.; Karnik, R.; Yue, M.; Li, D. Y.; Majumdar, A.; Yang, P. D. *Nano Letters* **2005**, *5*, 1633-1637.
(250) Austin, R. *Nature materials* **2003**, *2*, 567-568.
(251) Storm, A. J.; Chen, J. H.; Zandbergen, H. W.; Dekker, C. *Physical Review E* **2005**, *71*.
(252) Akeson, M.; Branton, D.; Kasianowicz, J. J.; Brandin, E.; Deamer, D. W. *Biophysical Journal* **1999**, *77*, 3227-3233.
(253) Mathe, J.; Aksimentiev, A.; Nelson, D. R.; Schulten, K.; Meller, A. *Proceedings of the National Academy of Sciences of the United States of America* **2005**, *102*, 12377-12382.
(254) Keyser, U. F.; Koeleman, B. N.; Van Dorp, S.; Krapf, D.; Smeets, R. M. M.; Lemay, S. G.; Dekker, N. H.; Dekker, C. *Nature Physics* **2006**, *2*, 473-477.
(255) Gracheva, M. E.; Xiong, A. L.; Aksimentiev, A.; Schulten, K.; Timp, G.; Leburton, J. P. *Nanotechnology* **2006**, *17*, 622-633.
(256) Lagerqvist, J.; Zwolak, M.; Di Ventra, M. *Nano Letters* **2006**, *6*, 779-782.
(257) Zhang, X. G.; Krstic, P. S.; Zikic, R.; Wells, J. C.; Fuentes-Cabrera, M. *Biophysical Journal* **2006**, *91*, L4-L6.
(258) Daiguji, H.; Oka, Y.; Shirono, K. *Nano Letters* **2005**, *5*, 2274-2280.
(259) Gijs, M. A. M. *Nature nanotechnology* **2007**, *2*, 268-270.
(260) Lee, C. S.; Blanchard, W. C.; Wu, C. T. *Analytical Chemistry* **1990**, *62*, 1550-1552.
(261) Schasfoort, R. B. M.; Schlautmann, S.; Hendrikse, L.; van den Berg, A. *Science* **1999**, *286*, 942-945.
(262) Ho, C.; Qiao, R.; Heng, J. B.; Chatterjee, A.; Timp, R. J.; Aluru, N. R.; Timp, G. *Proceedings of the National Academy of Sciences of the United States of America* **2005**, *102*, 10445-10450.
(263) Karnik, R.; Duan, C. H.; Castelino, K.; Daiguji, H.; Majumdar, A. *Nano Letters* **2007**, *7*, 547-551.
(264) Karnik, R.; Castelino, K.; Duan, C. H.; Majumdar, A. *Nano Letters* **2006**, *6*, 1735-1740.
(265) Vlassiouk, I.; Siwy, Z. S. *Nano Letters* **2007**, *7*, 552-556.
(266) Wei, C.; Bard, A. J.; Feldberg, S. W. *Analytical Chemistry* **1997**, *69*, 4627-4633.
(267) Apel, P. Y.; Korchev, Y. E.; Siwy, Z.; Spohr, R.; Yoshida, M. *Nuclear Instruments & Methods in Physics Research Section B-Beam Interactions with Materials and Atoms* **2001**, *184*, 337-346.
(268) Chen, P.; Mitsui, T.; Farmer, D. B.; Golovchenko, J.; Gordon, R. G.; Branton, D. *Nano Letters* **2004**, *4*, 1333-1337.
(269) Siwy, Z.; Heins, E.; Harrell, C. C.; Kohli, P.; Martin, C. R. *Journal of the American Chemical Society* **2004**, *126*, 10850-10851.
(270) Cervera, J.; Schiedt, B.; Ramirez, P. *Europhysics Letters* **2005**, *71*, 35-41.
(271) Miedema, H.; Vrouenraets, M.; Wierenga, J.; Meijberg, W.; Robillard, G.; Eisenberg, B. *Nano Letters* **2007**, *7*, 2886-2891.
(272) Sinha, P. M.; Valco, G.; Sharma, S.; Liu, X. W.; Ferrari, M. *Nanotechnology* **2004**, *15*, S585-S589.
(273) Martin, F.; Walczak, R.; Boiarski, A.; Cohen, M.; West, T.; Cosentino, C.; Ferrari, M. *Journal of Controlled Release* **2005**, *102*, 123-133.
(274) Gersborg-Hansen, M.; Balslev, S.; Mortensen, N. A.; Kristensen, A. *Microelectronic Engineering* **2005**, *78-79*, 185-189.
(275) Daiguji, H.; Yang, P. D.; Szeri, A. J.; Majumdar, A. *Nano Letters* **2004**, *4*, 2315-2321.
(276) Daiguji, H.; Oka, Y.; Adachi, T.; Shirono, K. *Electrochemistry Communications* **2006**, *8*, 1796-1800.
(277) van der Heyden, F. H. J.; Bonthuis, D. J.; Stein, D.; Meyer, C.; Dekker, C. *Nano Letters* **2006**, *6*, 2232-2237.

(278) van der Heyden, F. H. J.; Bonthuis, D. J.; Stein, D.; Meyer, C.; Dekker, C. *Nano Letters* **2007**, *7*, 1022-1025.
(279) Pennathur, S.; Eijkel, J. C. T.; van den Berg, A. *Lab on a Chip* **2007**, *7*, 1234-1237.
(280) Liu, S. R.; Pu, Q. S.; Gao, L.; Korzeniewski, C.; Matzke, C. *Nano Letters* **2005**, *5*, 1389-1393.